Petroleum Science 23 (2026) 563–581

Contents lists available at ScienceDirect

Petroleum Science

journal homepage: www.keaipublishing.com/en/journals/petroleum-science

Review Paper

The development of deformation bands from experiments: Review and perspective

Ming-Ming Jiang [a], Xiao-Fei Fu [b], Quan-You Liu [a,*]

[a] Institute of Energy, Peking University, Beijing, 100871, China
[b] State Key Laboratory of Continental Shale Oil, Northeast Petroleum University, Daqing, 163318, Heilongjiang, China

ARTICLE INFO

Article history:
Received 12 April 2025
Received in revised form
10 August 2025
Accepted 15 September 2025
Available online 20 September 2025

Edited by Xi Zhang and Jie Hao

Keywords:
Fault
Deformation bands
Subseismic faults
Experiment
Ring shear
Permeability
Simulation

ABSTRACT

Deformation band research has long been hindered by limited understanding of structural characteristics and physical properties during actual deformation processes. To address these knowledge gaps, this study systematically reviews experimental simulation methodologies through integrated approaches. Combining field observations with our newly developed ring shear tests for consolidated rocks, we investigate: formation mechanisms of deformation bands; key controlling factors including effective normal stress, shear displacement, clay content, mineral composition, porosity, particle size distribution, sorting, and cementation; comparative evaluation of experimental techniques (ring shear vs. direct shear vs. triaxial shear vs. sandbox modeling). Our analysis reveals two critical experimental parameters: effective normal stress and shear displacement. Notably, the advancement of consolidated rock-specific ring shear apparatus enables centimeter-scale displacement simulations, significantly enhancing deformation band experimentation. Current challenges in field measurement, image analysis, and 3D modeling are discussed with proposed solutions. Future directions emphasize: in-situ permeability testing, quantitative analysis frameworks, cementation dynamics, and numerical simulation optimization. This work aims to highlight deformation bands' crucial role in fluid migration and reservoir preservation while providing methodological guidance for designing simulation experiments. The compiled experimental protocols and analytical techniques offer researchers a systematic reference for deformation band investigations.

1. Introduction

With the gradual refinement and focus of exploration and development, the impact of small displacement faults on oil-water-gas separation, and oil-gas driving efficiency has garnered significant scholarly attention (Aydin, 1978; Aydin and Johnson, 1978; Sigda et al., 1999; Fossen and Hesthammer, 2000; Skurtveit et al., 2015; Jin et al., 2023; Fu et al., 2024; Gong et al., 2024; Jiang et al., 2024, 2025). It predominantly occurs within porous sandstone and carbonate rocks, with throw typically smaller than the thickness of the sandstone formation (Baud et al., 2004; Torabi et al., 2007; Ballas et al., 2012; Cheung et al., 2012; Soliva et al., 2016; Del Sole et al., 2020). The self-juxtaposition of sandstone in the same layer is formed, and it still has certain sealing ability due to the impact of cataclasis and compaction (Crawford, 1998; Gibson, 1994; Labaume and Moretti, 2001; Dewhurst and Jones, 2002; Pei et al., 2015).

Sandstones with varying porosity exhibit distinct types of subseismic faults (Maerten et al., 2006; Fossen et al., 2007; Fossen and Cavalcante, 2017; Rotevatn and Fossen, 2011; Balsamo et al., 2024). Rocks with low or non-porosity (<15%) are often subjected to force-induced fracturing, resulting in the formation of cracks and joints (Gong et al., 2021a, 2021b, 2023; Zeng et al., 2022; Du et al., 2023a; Laubach et al., 2023). These faults possess high porosity and permeability, facilitating fluid flow (Matthäi et al., 1998; Tindall, 2006, 2014; Tindall and Eckert, 2015; De Souza et al., 2021). Conversely, rocks with high porosity (porosity >15%) are more prone to developing deformation bands through cataclasis under force, which exhibit lower physical properties compared to the host rock and impede fluid flow (Fisher et al., 2003; Fossen and Bale, 2007; Ballas et al., 2013; Antonellini et al., 2014; Del Sole et al., 2020; Berge et al., 2022). Currently,

* Corresponding author.
E-mail address: liuqy@pku.edu.cn (Q.-Y. Liu).
Peer review under the responsibility of China University of Petroleum (Beijing).

https://doi.org/10.1016/j.petsci.2025.09.029

there have been numerous studies internationally on the impact of fractures and joints formed by low or non-porous rocks on oil and gas exploration and development (Compton et al., 2017; Fang et al., 2017; Schultz, 2019; Braathen et al., 2020; Du et al., 2023b; Torabi et al., 2023). However, research on the influence of deformation bands formed by high-porosity rocks is lacking primarily due to a dearth of physical simulation experimental methods for studying their formation and evolution under in-situ geological conditions (Jiang et al., 2023, 2024). Consequently, there exists an insufficient systematic understanding regarding the controlling factors influencing deformation bands as well as their sealing ability (Ballas et al., 2015; Soliva et al., 2016; Fossen et al., 2018).

The limitations in understanding deformation bands primarily arise from two issues. Firstly, the actual formation process of deformation bands is difficult to comprehend due to previous studies being based on observations and analyses of outcrops or cores, resulting in characteristics under static conditions without time continuity (Aydin and Reches, 1982; Lindsay et al., 1992; Antonellini et al., 1999; Hesthammer and Fossen, 1999; Fossen and Hesthammer, 2000; Berg and Skar, 2005; Davies et al., 2009; Childs et al., 2007; Cilona et al., 2012; Hennings et al., 2012; Chemenda et al., 2014; Liu Z. et al., 2021; Alkhasli et al., 2022). It is challenging to describe the continuous change process of deformation band formation in space. Although there are abundant researches on structural physics simulation experiments that simulate fault formation at all levels, experimental materials are mostly unconsolidated sediments (Clausen and Gabrielsen, 2002; Chuhan et al., 2003; Fukuoka et al., 2006; Torabi et al., 2007; Cuisiat and Skurtveit, 2010; Kimura et al., 2018, 2020; Zhu et al., 2022). Secondly, quantitative study of the main influence factors on the structure and physical properties of deformation bands remains a challenge. Existing field outcrop data can provide information about the structure and physical properties of deformation bands as well as other influencing factors (effective normal stress, shear displacement, etc.), but they result from joint control under various factors (Cuisiat and Skurtveit, 2010; Scibek, 2020; Ballas et al., 2015; Alkhasli et al., 2022; Ali et al., 2022; Balsamo et al., 2024). Previous studies only consider directly measurable single-factor influences such as displacement on cataclastic deformation band characteristics with defects that structural characteristics less than 10 μm cannot be measured comprehensively enough for a complete understanding of their formation and evolution or establishing a quantitative study (Beeler et al., 1996; Tikoff and Wojtal, 1999; Wibberley et al., 1999; Exner and Grasemann, 2010; Pizzati et al., 2020; Jiang et al., 2023).

Therefore, in order to effectively address the aforementioned issues, it is imperative to gain a comprehensive understanding of the current dynamics and advancements in research on experimental simulation deformation bands, as well as identify areas for future improvement. Building upon previous field and experimental findings, along with our own conducted ring shear tests applicable to consolidated rock, this paper primarily focuses on elucidating the formation mechanism of deformation bands and examining the existing research status regarding influential factors such as effective normal stress, shear displacement, clay content, mineral composition, porosity, particle size and sorting, as well as cements which impact the structure and physical properties of deformation bands. Simultaneously, a comparative analysis is conducted on various methods employed for studying deformation bands or fault zones including ring shear testing, direct shear testing triaxial shear testing sandbox experiments. Furthermore, the paper discusses prevailing challenges associated with field measurements, image analysis technology, and 3D model analysis technology used in analyzing deformation bands while proposing potential solutions. Finally, the study delves into future prospects encompassing elevated levels of investigation such as in-situ permeability testing of consolidated rock, quantitative analysis technology, cement selection and utilization, numerical simulation models, model setting, and application. This paper aims to highlight the significance of deformation bands and fault zones in fluid flow and preservation. It also seeks to provide researchers with clear and practical guidance on experimental methods and analytical techniques for studying these structures when designing simulation experiments and analyses. Simultaneously, it is anticipated that this study will foster increased interest in fundamental research on the structure and physical properties of deformation bands, as well as applied research aimed at enhancing the efficiency of oil and gas exploration and development in future endeavors.

2. Overview of the deformation mechanisms of deformation bands

Deformation bands are small-scale structures of influencing fluid flow in sandstone reservoirs (Fossen and Bale, 2007; Rotevatn et al., 2013; Tindall, 2014; Del Sole et al., 2020; De Souza et al., 2022; Berge et al., 2022). As a type of small displacement fault (subseismic fault, recessive fault) (Fisher et al., 2003; Parnell et al., 2004; Fossen and Bale, 2007; Ballas et al., 2012; Tueckmantel et al., 2012; Fossen et al., 2018), deformation bands can impede fluid flow both during geological history and in the development period of geological storage and its modeling (Fisher and Knipe, 2001; Flodin et al., 2003; Ballas et al., 2015). Deformation band refers to a distinctive banded structure that forms within porous sandstone through processes of compaction, expansion, and shearing, involving the rolling, rotation, and crushing of particles (Oda and Kazama, 1998; Baud et al., 2004; Fossen, 2010; Klimczak and Schultz, 2013; Ballas et al., 2015; Fossen et al., 2018; Brandes et al., 2022). Depending on variations in clay content and burial depth conditions, the deformation band can be categorized into three bands: disaggregation bands (clay content <15% and buried depth <1 km) (Fig. 1(a)), cataclastic bands (clay content <15% and buried depth 1–3 km) (Fig. 1(b)), and phyllosilicate bands (clay content 15%–40%) (Fig. 1(c)) (Fossen, 2010; Fossen et al., 2018).

Before the concept of deformation bands was defined, they were also referred to as fault zones or shear zones (Mandl et al., 1977; Caine et al., 1996; Childs et al., 1997; Mair et al., 2002; Wafid Agung et al., 2004; Fukuoka et al., 2006; Fossen and Cavalcante, 2017; Kimura et al., 2018). Previous experiments focused on loose sediment as the research object (Chuhan et al., 2003; Torabi et al., 2007; Cuisiat and Skurtveit, 2010). When the scale of the experiment is relatively small, such as in ring shear experiments, it is more commonly referred to as a shear zone (Mandl et al., 1977; Torabi et al., 2007; Cuisiat and Skurtveit, 2010). However, when the scale of the experiment is larger, such as in sand box experiments, it is more commonly called a fault zone (Childs et al., 2009; Balsamo and Storti, 2010; Scibek, 2020; De Souza et al., 2021). Therefore, although most experiments study fault zones and shear zones separately, they are essentially composed of the same type of material from a deformation mechanism perspective. In other words, a shear zone represents one type of deformation band while a deformation band represents one type of fault zone; another type being clay smear zones.

Cataclastic deformation bands are commonly observed in various regions, including the Songliao Basin (Meng et al., 2014; Liu B. et al., 2021), Bohai Bay Basin (Liu Z. et al., 2021; Jin et al., 2023; Gong et al., 2024), Qaidam Basin (Liu and Sun, 2020; Pei et al., 2020), and Jianghan Basin in China; the Crotone Basin in Italy (Balsamo and Storti, 2010; Pizzati et al., 2020); the Vienna Basin in Austria (Exner et al., 2013; Lommatzsch et al., 2015); and

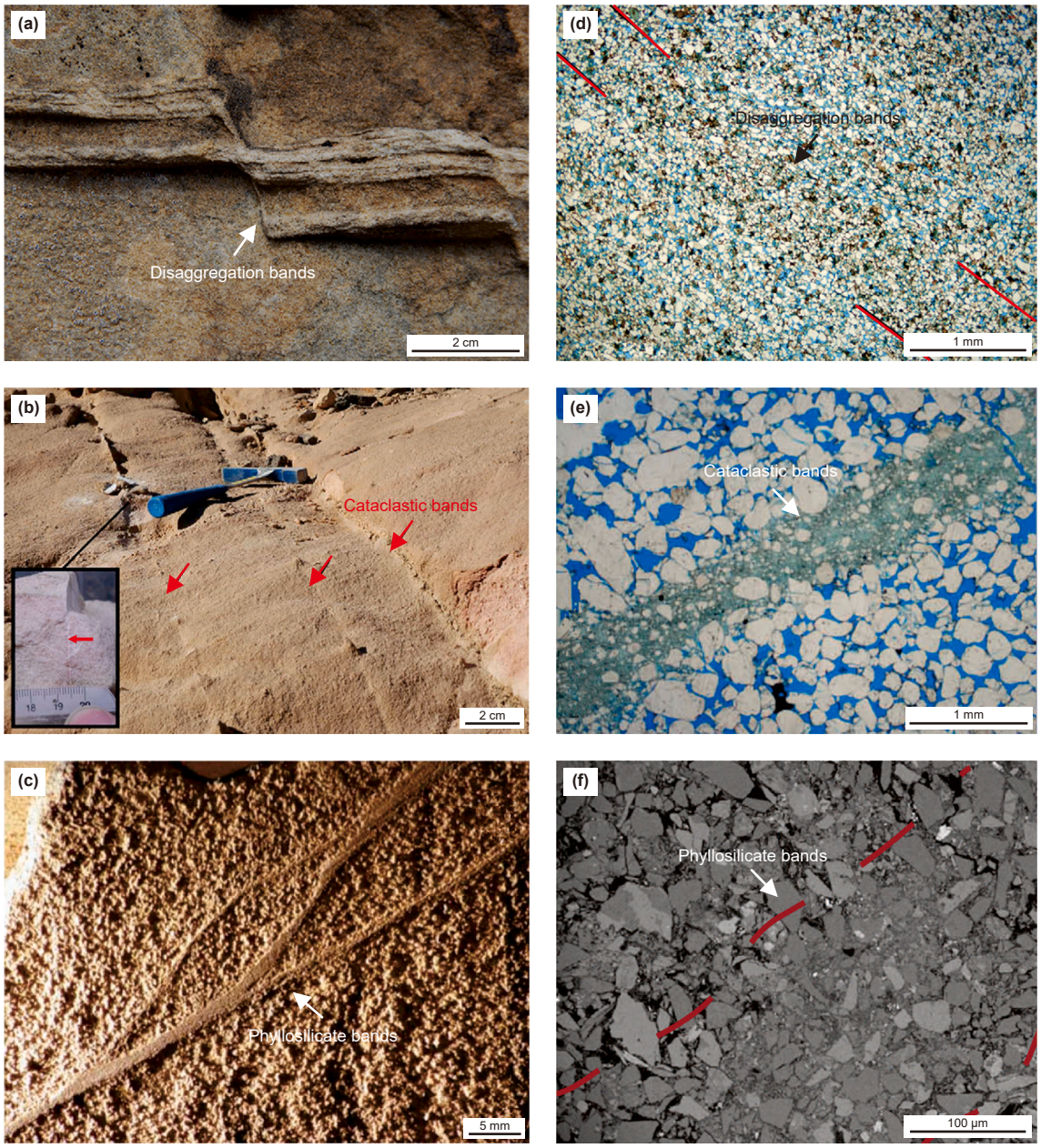

Fig. 1. Major classification of deformation bands. **(a)** Disaggregation bands, **(b)** cataclastic bands, and **(c)** phyllosilicate bands are macroscopic features. **(d)** Disaggregation bands, **(e)** cataclastic bands, and **(f)** phyllosilicate bands are microscopic features. Modified from Ballas et al. (2015) and Fossen (2010).

the Rio do Peixe Basin in Brazil (Araujo et al., 2018; Nicchio et al., 2018; De Souza et al., 2021; Oliveira et al., 2022; Silva et al., 2022). These bands typically form under different tectonic stress fields. For instance, cataclastic deformation bands developed within the Youshashan structural belts of the Qaidam Basin are formed within reverse fault zones under compressional environments. On the other hand, those within the Xicaogu structural belts of Bohai Bay Basin form within normal fault zones under extensional environments (Liu and Sun, 2020; Liu Z. et al., 2021). Generally, cataclastic deformation bands formed by normal faulting exhibit a more significant reduction in permeability compared to those formed by reverse faulting (Ballas et al., 2015). Furthermore, cataclastic deformation bands tend to be more prevalent at medium burial depths (<1 km), where permeability reduction is greater than that observed at shallow burial depths (1–3 km) or deep burial depths (>3 km) (Ballas et al., 2015).

3. Main factors affecting the deformation bands

The structure and physical properties of deformation bands formed under different conditions exhibit variations (Fossen et al., 2007, 2018; Ballas et al., 2015; Ali et al., 2022; Jiang et al., 2022, 2023, 2024). This can be attributed to the influence of external geological factors, such as stress and displacement, as well as internal factors related to the host rock, including clay content, mineral composition, porosity, particle size distribution, and cementation (Ballas et al., 2015; Soliva et al., 2016; Fossen et al., 2018; Pizzati et al., 2020; Jiang et al., 2023, 2024).

3.1. Effective normal stress

The effective normal stress is a crucial factor directly influencing rock deformation (Fossen et al., 2007, 2018; Ballas et al., 2015). At low stress levels, particle deformation occurs through edge spalling, while at high stress levels, it takes place via particle cataclasis. In other words, as the effective normal stress increases, the shear stress experienced by the sliding shear plane of the fault intensifies and cataclasis becomes more pronounced (Torabi et al., 2007; Kimura et al., 2018). This will be a reduction in particle size and sorting (Engelder, 1974; Takahashi, 2003; Fossen et al., 2007, 2018; Fukuoka et al., 2007), accompanied by an increase in the thickness of the deformation band (Torabi et al., 2007; Kimura et al., 2018, 2020; De Souza et al., 2021). Consequently, there will be a decrease in both porosity and permeability (Kaproth et al., 2016; Fisher et al., 2018). When all other factors remain constant, an increase in stress exhibits a positive correlation with cataclasis intensity (Fig. 2). However, permeability may not always decrease accordingly. Notably, when stress reaches 2–3 MPa, both cataclasis and permeability undergo significant changes (Kimura et al., 2014, 2018, 2020; Jiang et al., 2023). When the stress increased by 8 MPa, there was an observed increase in cataclasis, accompanied by a simultaneous decrease in permeability (Kimura et al., 2018, 2020). Furthermore, when all other factors remain unchanged, the impact of stress on physical properties may have one or multiple critical values. Considering that permeability is highly sensitive to stress and that cataclastic deformation bands form under shallow burial conditions (Fossen et al., 2018), it is generally advisable to avoid excessively high stresses. The distinction between stresses above or below critical values regarding their influence on the structure and physical properties of cataclastic deformation bands should not be overlooked.

3.2. Shear displacement

In the field of structural geology, extensive research has been conducted on the impact of displacement, also known as fault throw or shear displacement, on the formation and evolution of deformation bands (Pickering et al., 1997; Exner and Grasemann, 2010; Choi et al., 2016; Pizzati et al., 2020). These bands can be directly observed and measured in outcrop studies. Early experiments revealed that an increase in displacement along the shear direction leads to a decrease in particle size and sorting of cataclastic particles (Engelder, 1974; Torabi et al., 2007). The subsequent experiments and field outcrop observations revealed that displacement led to an intensified cataclasis of particles, resulting in a reduction in permeability and an increase in the thickness of deformation bands (Du Bernard et al., 2002; Balsamo and Storti, 2010; Kaproth et al., 2016; Kimura et al., 2018; Pizzati et al., 2020). However, once a certain degree of displacement is reached, there will be no further changes in particle size, permeability, and thickness of deformation bands (Fig. 3) (Childs et al., 2009; Sadrekarimi and Olson, 2010; Nicol and Childs, 2018). The subsequent variations will be contingent upon the magnitude of the applied stress (Kimura et al., 2014, 2018). When displacement is small, particles undergo reorientation with minimal cataclastic intensity. On the other hand, when displacement is large, fault core develop within the inner zone of cataclastic deformation bands

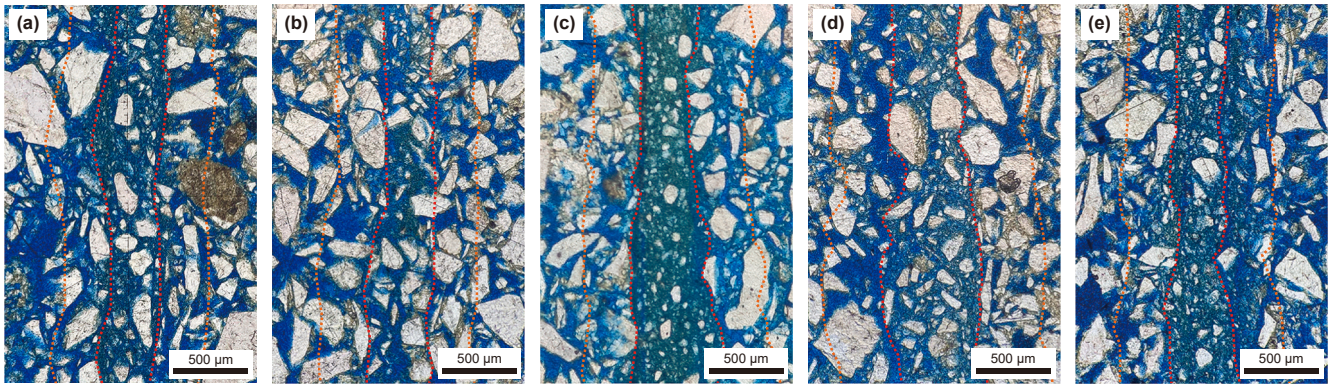

Fig. 2. Microstructures of cataclasis under different stress conditions. Modified from Jiang et al. (2023). Experimental conditions with effective normal stress of **(a)** 1 MPa, **(b)** 1.5 MPa, **(c)** 2 MPa, **(d)** 2.5 MPa, and **(e)** 3 MPa and rotational angels of 90°. Experimental details (including instrumentation, procedures, and testing methods) are provided in the Supplementary material.

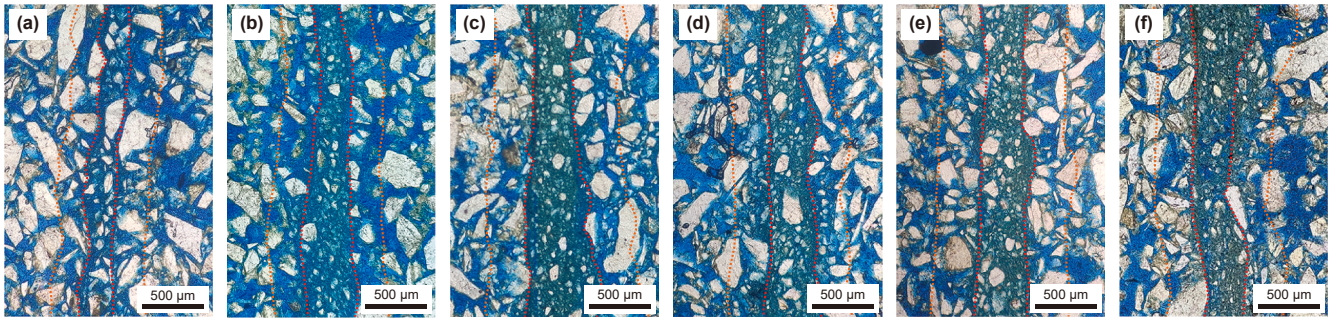

Fig. 3. Microstructural evolution of cataclasis with varying displacement. Modified from Jiang et al. (2023). Experimental conditions with rotational angels of **(a)** 30°, **(b)** 60°, **(c)** 90°, **(d)** 120°, **(e)** 150°, and **(f)** 190° and effective normal stress of 2 MPa. Experimental details (including instrumentation, procedures, and testing methods) are provided in the Supplementary material.

resulting in a dark matrix appearance (Pizzati et al., 2020). And particle size reduction is not significant in the outer zone. Additionally, tensile cracks parallel or inclined to the shear direction may appear. In a general sense, increasing displacement leads to increased shear strain which affects deformed structures and reduces permeability, and the influence on permeability due to shear strain remains limited (Kaproth et al., 2016; Kimura et al., 2018). Therefore, it is crucial to understand how different shallow burial stress conditions affect increases in displacement without impacting structure and physical properties of cataclastic deformation bands; this aspect currently lacks clarity.

3.3. Clay content

The clay content in the host rock will influence the frictional strength during deformation and play a regulatory role in shear forces, inhibiting cataclasis (Takahashi et al., 2007; Cuisiat and Skurtveit, 2010; Dimitrova and Yanful, 2012; Tesei et al., 2017; Nicol and Childs, 2018; Zhang et al., 2019). Experimental findings indicate that when the clay content ranges from 0% to 50%, the measured permeability value decreases by 2–6 orders of magnitude (Fig. 4). Moreover, with an increase in clay content and shear strain, the corresponding permeability also decreases or stabilizes (Crawford et al., 2001, 2008). Various experiments conducted by scholars have identified different critical points for changes in permeability or frictional strength at either 25% (Takahashi et al., 2007) or 15% (Zhang et al., 2019) clay content due to variations in experimental methods and conditions. The permeability is highly sensitive to the clay content (Kaproth et al., 2016). It is worth noting that a significant number of field outcrop studies define a clay content range of 0%–15% as critical for cataclastic deformation band formation (Fossen et al., 2007, 2018). However, further research is required to understand the differential impact of changing clay content within this specific interval on structural and physical properties.

These findings highlight the necessity for careful control of clay content in experimental design. As demonstrated by Crawford et al. (2008), systematic variation of kaolinite content in quartz-rich gouge mixtures, combined with triaxial shear testing and pore pressure oscillation techniques, allowed for high-resolution monitoring of permeability changes across a broad compositional spectrum. Their use of well-mixed synthetic gouge layers, precise loading paths, and fluid substitution protocols (e.g., switching from water to argon) illustrates a robust experimental framework for assessing how clay content regulates fault zone hydromechanical properties. Inspired by this approach, future deformation band experiments should incorporate similar compositional gradients and instrumentation to accurately capture permeability thresholds and mechanical transitions driven by clay content.

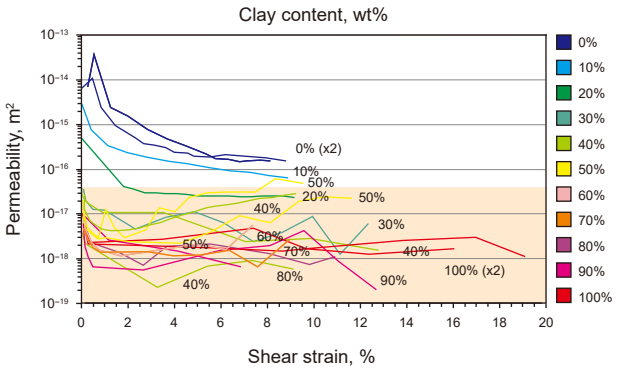

Fig. 4. Relationship between permeability of fault rocks and shear strain under different clay contents. Modified from Crawford et al. (2008, 2001).

3.4. Mineral composition of the host rock

The mineral composition and particle strength of the host rock exert influence on the mechanism of particle cataclasis within deformation bands (Rawling and Goodwin, 2003; Fossen et al., 2007; Cooke et al., 2018). Quartz and feldspar are significant constituents in porous sandstone, but their deformation behaviors differ substantially. Quartz exhibits higher grain strength compared to feldspar, undergoing grain edge spalling while transgranular fracture is rarely observed (Fig. 5(a)). Conversely, feldspar readily undergoes cleavage-induced transgranular fracture, resulting in the formation of smaller clastic particles (Fig. 5(b)) (Rawling and Goodwin, 2003; Pizzati et al., 2020). Ring shear experiments have revealed that mineral crystal shape also impacts fault permeability. Single crystal quartz-feldspathic particles exhibit a rounded shape, with increasing displacement leading to enhanced cataclasis and shear localization, ultimately developing distinct layered structures characterized by low permeability layers juxtaposed with high permeability layers within the deformation band (Fig. 6(a)). On the other hand, single crystal muscovite particles possess a platy morphology. As displacement increases, initially oriented muscovite particles begin rotating extensively and numerous P and R fractures develop between them (Fig. 6(b)). Consequently, the permeability anisotropy of the deformation band formed by muscovite is lower than that of quartz-feldspar gouge (Zhang et al., 1999). While both quartz-dominated and feldspar-dominated sandstones can generate cataclastic deformation bands through cataclasis processes, specific differences in structure and physical properties after deformation remain to be determined.

3.5. Porosity of the host rock

The stress at the contact point between particles increases with porosity, promoting cataclasis and reducing permeability (Flodin et al., 2003; Kimura et al., 2014, 2018; Cooke et al., 2018). However, in the absence of faults and shallow burial depths, high-porosity sandstone experiences less reduction in permeability than medium-porosity sandstone within deformation bands (Fossen et al., 2007; Ballas et al., 2015). In other words, the role of porosity in sandstone deformation is fundamentally influenced by structural mechanisms and burial depth. Thus, porosity only serves as a secondary factor affecting cataclastic deformation band formation.

3.6. Particle size and sorting of the host rock

Particle size and sorting of the host rock are also factors that influence the formation of deformation bands and their permeability (Ballas et al., 2015; Cooke et al., 2018; Oliveira et al., 2022). The cataclasis intensity of particles depends on the original particle size of the host rock. Coarse sandstone exhibits a relatively higher cataclasis intensity compared to fine sandstone, resulting in a higher proportion of deformation bands with a decrease in permeability by more than two orders of magnitude (Fig. 7(a) and (b)). The impact of cataclasis intensity and permeability becomes more pronounced as particle size increases (Balsamo and Storti, 2010, 2011). However, when considering burial depth and tectonic mechanisms, there is no significant difference in permeability values between deformation bands formed in coarse and fine sandstone (Ballas et al., 2015). Therefore, it can be considered

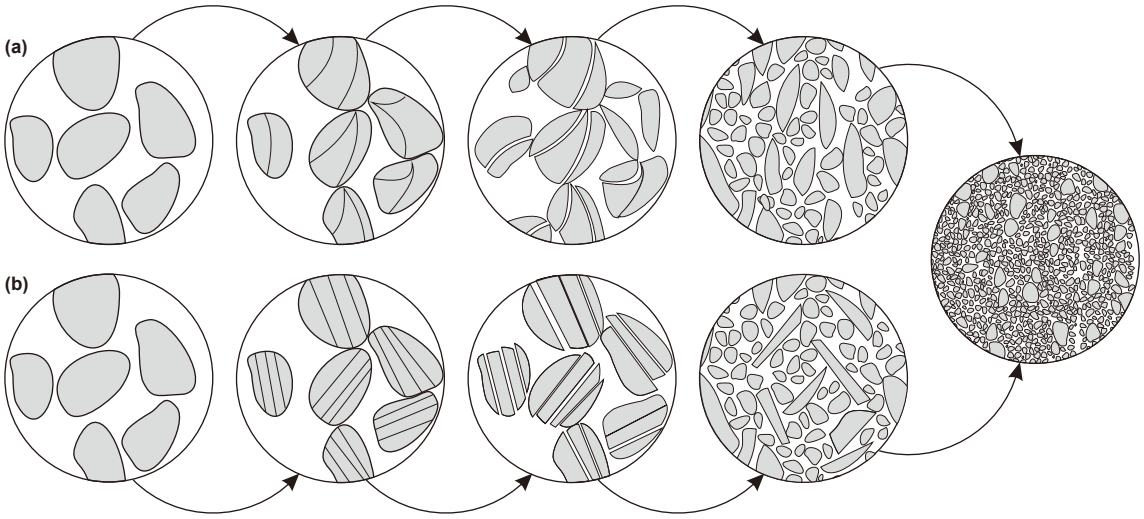

Fig. 5. Cataclastic mechanisms of different minerals. **(a)** Quartz, **(b)** feldspar.

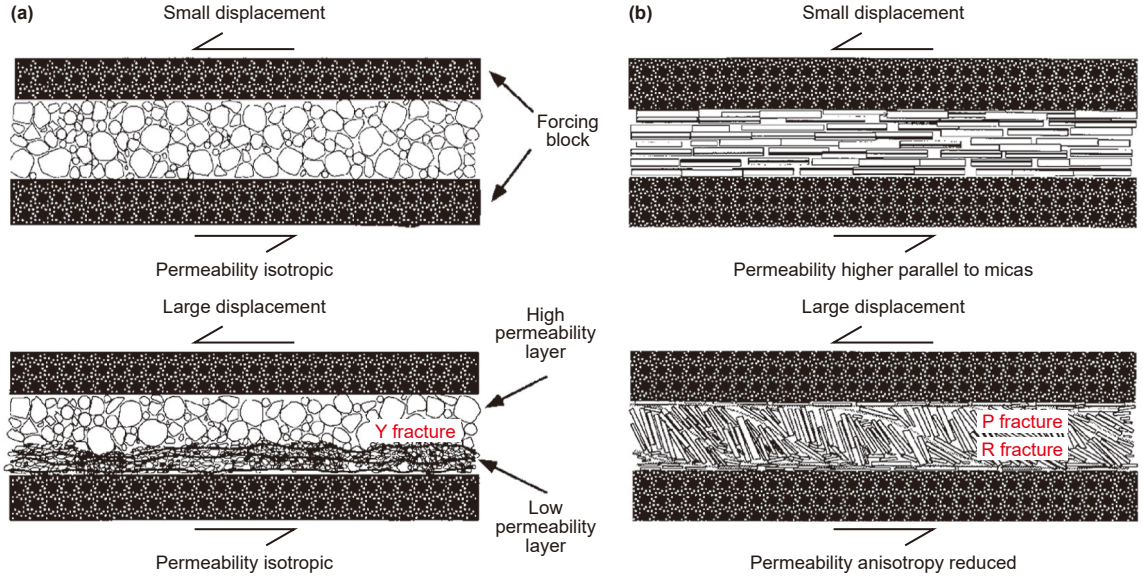

Fig. 6. Shear evolution models of fault gouge with different mineral compositions. **(a)** Quartz-feldspar gouge. **(b)** Muscovite gouge. Modified from Zhang et al. (1999).

as a secondary factor influencing the formation of cataclastic deformation bands.

The occurrence of cataclasis is more likely in particles of similar size, and the degree of sorting plays a crucial role in promoting cataclasis (Sammis et al., 1987; Cheung et al., 2012). Poor sorting will promote particle rearrangement, and cataclasis will preferentially occur in small particles (Fig. 7(c) and (d)) (Solum et al., 2010; Cheung et al., 2012; Ballas et al., 2015). This is because angular particles possess a higher internal friction angle compared to rounder particles, which significantly influences the shearing and friction processes (Klinkmüller et al., 2016). Consequently, good sorting has a greater impact on permeability within the cataclastic structure; however, this effect still depends on the presence of large faults or their burial depth conditions. The magnitude of stress amplifies this effect, leading to the formation of cataclastic deformation bands in shallowly buried regions (Ballas et al., 2015). It should be noted that while sorting does have some influence on the development of cataclastic deformation bands, its significance remains relatively minor.

3.7. Cementation

Cementation generally occurs under two conditions. One condition is the presence of carbonate minerals, such as calcite and dolomite, in the host rock with a high content (Exner et al., 2013; Skurtveit et al., 2015; Pizzati et al., 2020). The other is influenced by groundwater, hydrocarbons, and various fluid substances (Mozley and Goodwin, 1995; Parnell et al., 2004). This process may occur concurrently or after deformation (Hodson et al., 2016), and its complex physicochemical nature necessitates comprehensive analysis by integrating burial history and thermal evolution history (Fossen et al., 2007). However, based on international case studies from field outcrop studies, there is limited evidence of cementation during the formation of cataclastic deformation

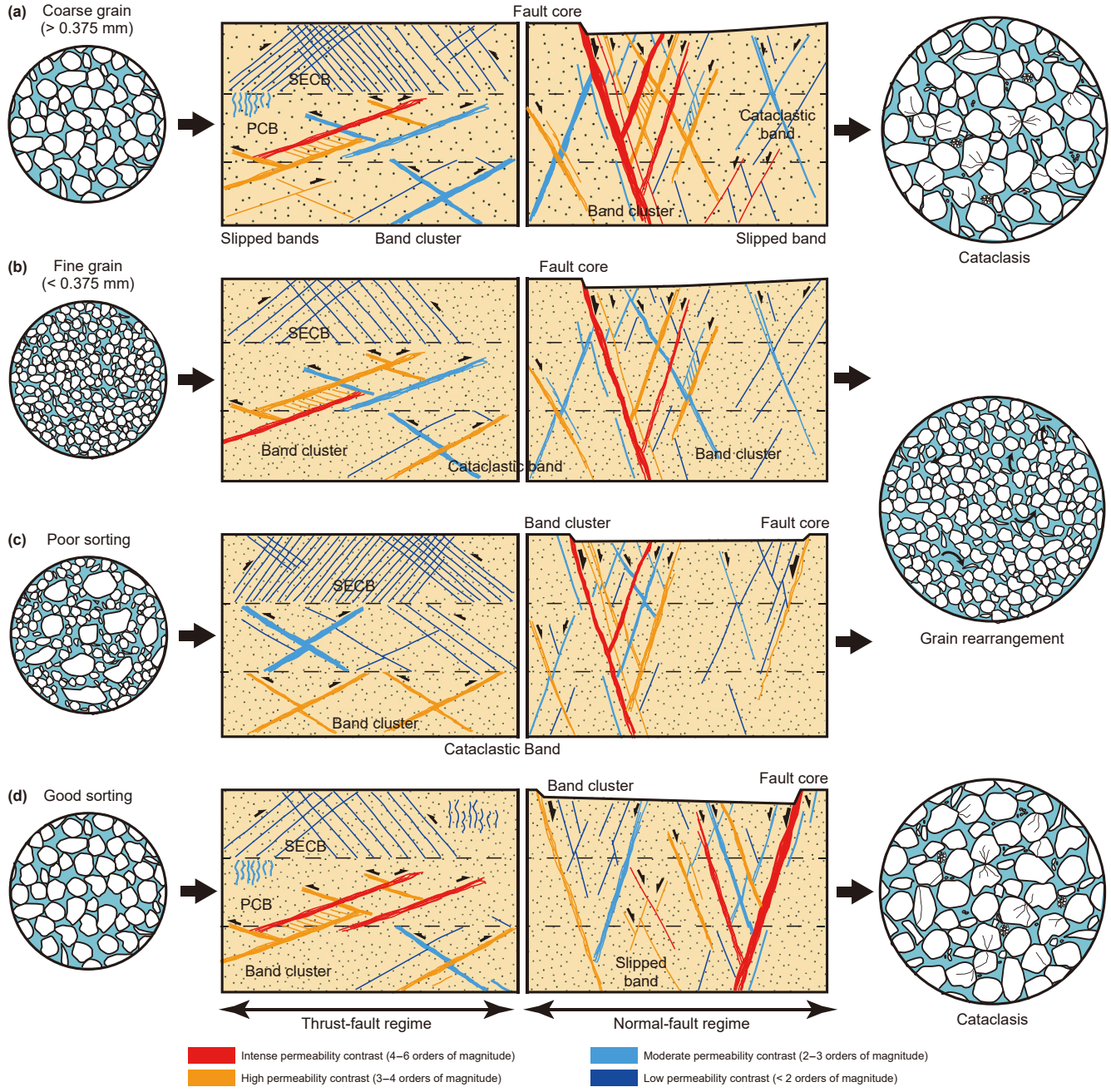

Fig. 7. Schematic diagram of permeability variation in cataclastic deformation bands influenced by particle size and sorting of host rocks. The particle size of the host rock is **(a)** coarse and **(b)** fine, respectively. The particle size sorting of the host rock was **(c)** poor and **(d)** good, respectively. Modified from Ballas et al. (2015).

bands (Del Sole et al., 2020; Skurtveit et al., 2015). The hindered cementation is attributed to the small pore volume resulting from significant cataclasis (Hodson et al., 2016).

In general, a significant number of outcrops and experimental studies pertaining to deformation bands indicate that the primary factors influencing their formation, structure, and physical properties are effective normal stress, shear displacement, strain rate, clay content, and mineral composition of the host rock within similar geological backgrounds (including lithology, particle size distribution, sorting characteristics, and porosity) (Figs. 8 and 9). Among these factors, effective normal stress and shear displacement emerge as the two most crucial determinants.

4. Experimental simulation methods

Currently, the international methods for simulating shear physics experiments include three types (Table 1): ring shear (Fig. 10(a)) (Cuisiat and Skurtveit, 2010; Kimura et al., 2020; Jiang et al., 2023, 2024), triaxial shear (Fig. 10(b)) (Crawford B. et al., 2002; Elkhoury et al., 2011), and direct shear (Fig. 10(c)) (Barla et al., 2010; Giger et al., 2013). Additionally, there is a saturated water sand box physical simulation experiment available. Numerous experimental studies can effectively correspond to outcrop phenomena and seismic data. During the process of conducting shear experiments, clay smear and other fault sealing

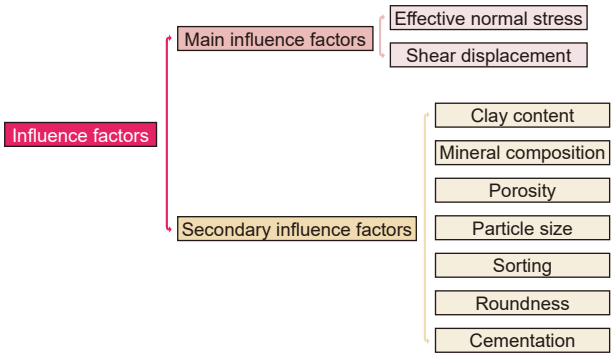

Fig. 8. Factors influencing the formation of deformation bands.

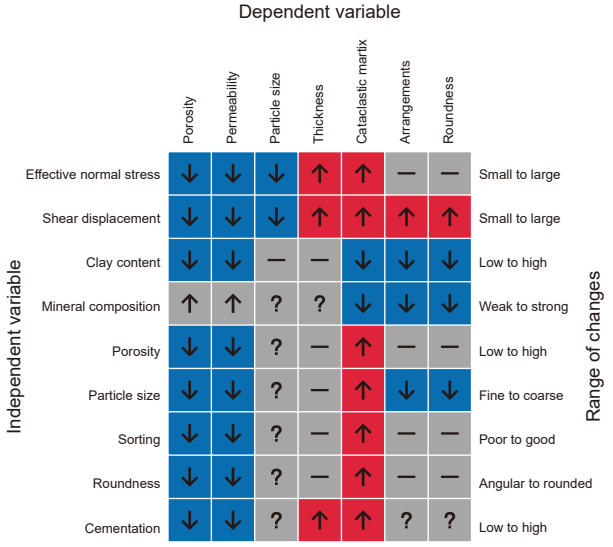

Fig. 9. Variations in deformation band structure and physical properties influenced by different factors. An upward arrow indicates an increase in the dependent variable with the independent variable, while a downward arrow denotes a decrease. A short line shows no change, and a question mark represents uncertain changes. Colors correspond to these trends: red (increase), blue (decrease), and grey (uncertain/requires confirmation).

types are investigated through forward modeling of fault formation processes. By adjusting experimental parameters, it is possible to simulate the formation of fault zones and even replicate in-situ conditions during fault formation.

4.1. Ring shear experiment

The advantage of the ring shear experimental device (Fig. 10(a)) lies in its capability to simulate centimeter-level displacements, multi-layer system conditions, and pure sandstone fault rocks (Cuisiat and Skurtveit, 2010). In this study, consolidated rock specimens were prepared from artificial sandstone (quartz 88.8%, clay minerals 11.2%, porosity 30.86%, permeability 1118.5 mD, uniaxial compressive strength 16.96 MPa) to ensure uniform host rock properties. The custom-built high-pressure, low-velocity ring-shear apparatus employed an annular sample cell (inner diameter 40 mm, outer diameter 75 mm, height 30 mm) accommodating fan-shaped specimens. Axial load was applied in constant-stress mode via a servo-controlled actuator, while rotational displacement was incrementally imposed by mechanical turning of the specimen sectors. Torque and axial force were monitored with a resolution of 0.01 N·m. PTFE liners minimized boundary friction and preserved sample integrity during shearing. Experimental control conditions included a shear rate of 50 μm/s and room temperature (18 °C), with variable effective normal stress (1–3 MPa) and rotation angle corresponding to shear displacements up to ~249 mm. Currently, research on ring shear experiments primarily focuses on loose sediments, investigating cataclasis intensity (Kimura et al., 2018, 2020), changes in physical properties (Jiang et al., 2024), and soil shear resistance (Ma et al., 2019; Zhu et al., 2022). However, there is a lack of design for consolidated rock specimens in these experiments, requiring more time and effort compared to other physical simulation studies. Although some experiments have been conducted on consolidated rock samples, further research is needed in the future.

4.2. Direct shear experiment

The advantage of a direct shear device (Fig. 10(c)) lies in its capability to achieve high stress loading on porous or composite rock masses, as well as conduct permeability measurements under fluid-sealed conditions. Based on different stress loading methods, it can be categorized into three types: vertical thrust type (Karakouzian and Hudyma, 2002), lateral compression double shear type (Main et al., 2001; Barla et al., 2010), and vertical compression type (Giger et al., 2011, 2013). The lateral compression double shear type is more commonly used. However, it is limited by the observation of local strain rather than overall changes in rock mechanics. The vertical compression type is a direct shear device suitable for large sample sizes that allows for fluid injection to study permeability changes and apply significant stresses. Nevertheless, there may be a deviation of 1–5 orders of magnitude (Giger et al., 2013). One limitation remains the inability to achieve centimeter-level displacements.

4.3. Triaxial shear experiment

The triaxial shear experiment (Fig. 10(b)) remains a cornerstone of laboratory-based fault zone research due to its ability to impose realistic stress conditions and monitor hydromechanical properties under controlled deformation (Crawford et al., 2008; Takahashi et al., 2007; Samuelson et al., 2009; Elkhoury et al., 2011). Its primary advantage lies in the simultaneous application of confining and pore pressures, allowing simulation of burial depth, pore-fluid presence, and effective stress evolution. Additionally, modern triaxial systems enable real-time measurement of parameters such as frictional strength, permeability, and volumetric strain, making them highly suitable for studying the formation and evolution of deformation bands. However, despite its strengths, the method faces several limitations. Shear displacement is often restricted to less than 20 mm, limiting its ability to simulate long-term strain localization or mature fault architectures. The simplified geometry of specimens and fixed loading configurations also constrain the replication of complex natural stress fields, such as true triaxial or anisotropic tectonic stresses.

Moreover, variations in experimental setups, such as differences in drainage conditions, pore fluid types, sample aspect ratios, and strain rates, can lead to significant discrepancies in measured permeability and mechanical thresholds, hindering result comparability across studies. For instance, undrained conditions may suppress compaction effects, whereas constant pore pressure conditions can obscure the impact of fluid diffusion on sealing efficiency. Similarly, strain rate sensitivity in clay-rich gouges can introduce nonlinear behavior not captured under faster displacement rates.

Table 1
Experimental equipment for shear physical simulation of fault rock.

Experimental device	Reference	Institution/ developer	Sample size & geometry	Max normal stress, MPa	Shear displacement, mm	Drainage/pore fluid system	Shear rate/ control	Permeability measurement method	Strengths	Limitations
Loose sediment direct shear	Karakouzian and Hudyma (2002)	University of Nevada	Cylindrical, $D = 50.8$ mm, $H = 102$ mm	Low	Up to 50	Undrained; video observation	1.6 mm/min motor drive	None reported	Simple, low-cost analog model	Cannot handle lithified rocks
Triaxial shear apparatus	Takahashi (2003)	Japan National Oil Corporation	Cylindrical, $D = 40$ mm, $H = 95$ mm	Up to 300	8 mm	Water; Oscillatory pressure method	Servo control, 1.0 μm/s	Real-time permeability	High stress/ temperature	Limited displacement, complex setup
High-pressure ring shear	Torabi et al. (2007)	Norwegian Geotechnical Institute & University of Bergen	Annular, $W = 25.4$ mm, $H = 45$ mm	Up to 20	Unlimited	Drainage valves top/ bottom	Rotation under constant σn/2°/ min	None reported	Simulates deep burial; residual strength analysis	Direct observation limited
True-triaxial shear	Ikari et al. (2009)	Pennsylvania State University	Layered, 4–5 mm thickness	12–59	1.2–2.5	Deionized water; pressure gradient	Servo-controlled, ±0.02 mm	Real-time permeability	Controls Pc, Pp, slip velocity precisely	Complex assembly; not real-time flow
High-pressure direct shear	Barla et al. (2010)	Polytechnic University of Turin	Cylindrical, $D = 50$/ 100 mm, $H = 50$ mm	Up to 10	Max 18	Back pressure via servo-controlled actuator system	Servo-controlled motors	None reported	Accurate force/ displacement tracking	Small displacement
Loose sediment ring shear	Sadrekarimi and Olson (2010)	University of Illinois	Annular; variable	Low	Unlimited	Global drainage	Variable via motor control	None reported	Large displacement; shear band dynamics; partially observed	No internal pore pressure data
Loose sediment ring shear	Cuisiat and Skurtveit (2010)	Norwegian Geotechnical Institute	Annular; variable	Up to 10.5	Up to 20	Unlimited	Drainage valves top/bottom	Real-time permeability	Simulates deep burial; residual strength analysis	Direct observation limited
Large-scale direct shear	Giger et al. (2011)	CSIRO, Australia	Up to 600 × 300 × 300 mm	Up to tens	~100+	Sealant-based dual-fluid system	0.26 mm/min to 2.2×10^5 m/s	Real-time flux tracking	Large rock samples, long displacement, sealing control	Complicated sealant calibration
High-pressure ring shear (new)	Jiang et al. (2023)	Northeast Petroleum University	Fan-shaped, $D = 40$–75 mm, $H = 30$ mm	Up to 50	~416	None	Up to 1 mm/min	After experiments	Large displacement, full-circle shear, programmable	Direct observation limited; Fluid sealing remains challenging

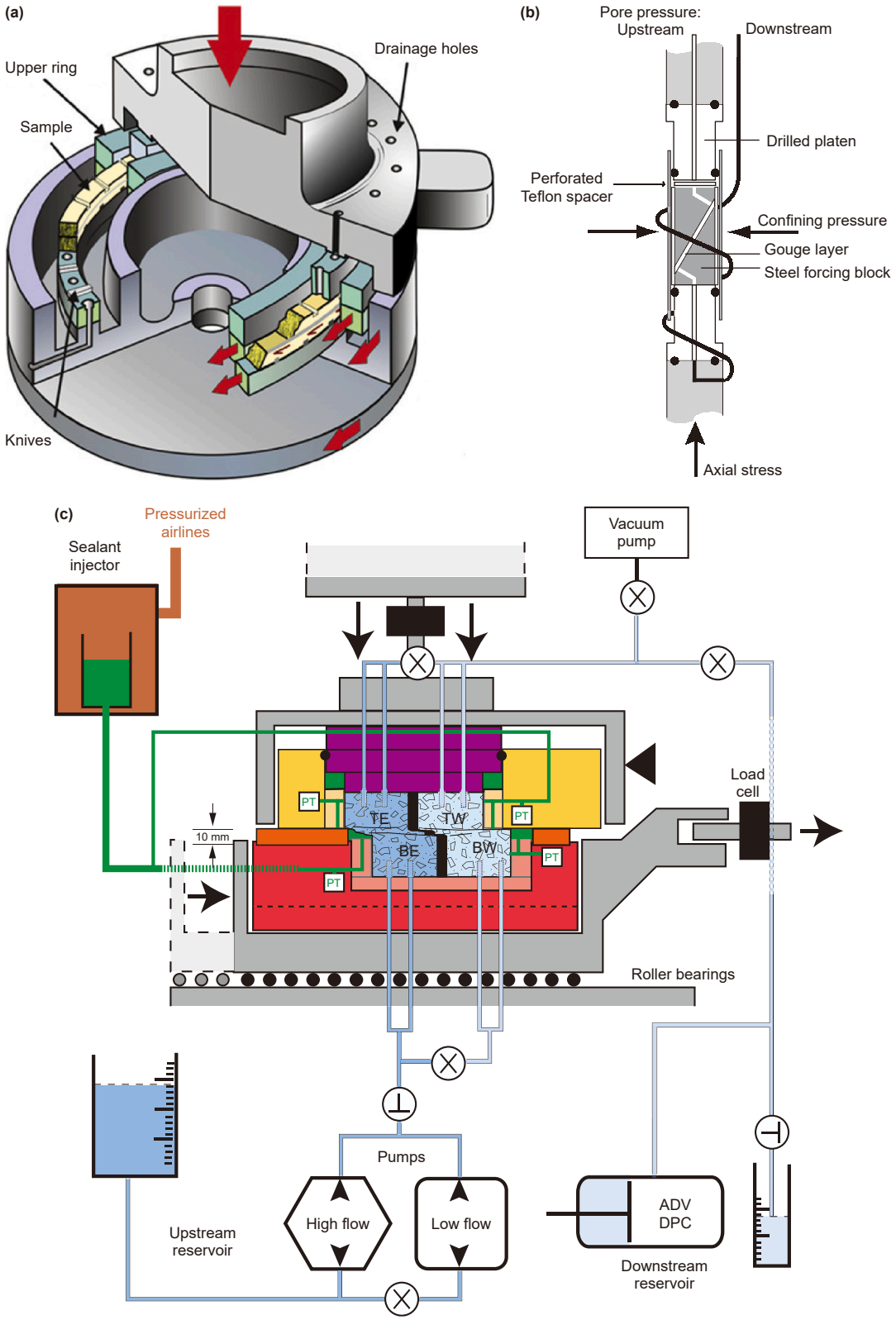

Fig. 10. Internationally representative shear simulation apparatus. **(a)** Ring shear apparatus, modified from Cuisiat and Skurtveit (2010). **(b)** Triaxial shear apparatus, modified from Crawford et al. (2002). **(c)** Direct shear apparatus, modified from Giger et al. (2013).

These limitations suggest that future triaxial experiments should prioritize modular designs that allow for flexible control of loading paths (e.g., independent σ_1-σ_2-σ_3 paths), variable shear displacement capacity, and standardized sample geometries. Integration with permeability monitoring techniques, such as pore pressure oscillation or pulse decay methods, under well-defined flow directions (e.g., parallel versus perpendicular to shear) will also enhance the reliability of data. By refining these aspects, triaxial shear experiments can more faithfully replicate the coupled mechanical and hydraulic processes occurring in natural deformation bands.

4.4. Sandbox experiment

In addition to the aforementioned physical simulation experiment on shear, there exists an alternative method for structural physical simulation that satisfies the similarity principle and sets boundary conditions to simulate basin structures and local tectonic deformation processes (Noorsalehi-Garakani et al., 2013). The direct observation of structural deformation makes this method highly applicable in the study of hydrocarbon accumulation and migration (Yan et al., 2021). However, this method also exhibits certain limitations, such as the utilization of loose quartz sand, microglass beads, and other materials that differ significantly from consolidated rock in experimental settings. Consequently, various factors may restrict the accuracy of experiments and produce errors.

In general, over time, scholars have successfully addressed various challenges such as direct observation of clay smear, stress loading control, millimeter displacement control, mechanical and permeability testing, fluid sealing, etc. However, there has been limited progress in enhancing experimental instruments for shear physical simulation in the past decade. Particularly lacking is experimental research on centimeter-level displacement of consolidated rock.

4.5. Comparison of experimental parameters

To systematically evaluate methodological trends and parameter-space coverage in laboratory studies of deformation band formation, a comparative summary of key experimental parameters is presented in Table 2. This synthesis includes effective normal stress, shear displacement, clay content, shear strain rate (in μm/s), and the associated permeability measurement techniques across representative studies. The effective normal stress applied in these experiments spans from sub-megapascal levels (e.g., Cuisiat and Skurtveit (2010): 0.7–10.5 MPa) to as high as 80 MPa (Takahashi et al., 2007), reflecting attempts to simulate near-surface to intermediate burial conditions. Shear displacement varies widely, from just a few millimeters to over 200 mm, depending on device design and material cohesion. Clay content, a critical factor in mechanical localization and sealing behavior, ranges from 0% to over 50%, though relatively few studies explore values beyond 30%.

Strain rate settings range from quasi-static (~0.2 μm/s) to relatively fast shearing (up to 100 μm/s), with most experiments conducted at constant displacement rates. Permeability measurement methods differ significantly, from real-time monitoring using pore pressure oscillation or steady-state flow (e.g., Crawford et al. (2008)) to post-deformation imaging or porosity analysis. These variations introduce limitations in direct cross-comparison and highlight the need for methodological standardization. Notably, while most experiments confirm that deformation bands tend to reduce permeability and often act as baffles or seals, the structural style (e.g., compaction vs. cataclasis vs. clay smear) and timing of localization (early vs. late during shearing) remain underexplored in high-clay-content or long-duration settings. This integrated dataset serves to identify key experimental trends, while also revealing gaps—particularly the lack of high-resolution, real-time permeability data under large displacement and elevated clay content scenarios.

5. Analytical methods

5.1. Measurements in field

The geological survey is the fundamental and pivotal task of geological exploration, wherein a significant portion of invaluable data is acquired through direct measurements of geological phenomena in the field. The methods primarily encompass measuring the dimensions (length and width) of deformation bands, determining the strike, dip, and inclination angle of faults associated with these deformation bands, quantifying their porosity and permeability characteristics, as well as documenting their macro distribution patterns and growth environments. Instruments employed for these measurements typically include small or large

Table 2
Experimental methods for shear physical simulation of fault rock.

Reference	Rock type/material	Effective normal stress, MPa	Shear displacement, mm	Clay content, %	Strain rate	Permeability measurement	Notes on band formation
Crawford et al. (2008)	Synthetic gouge (quartz + kaolinite)	5–50	~3	0–50	0.3 μm/s	During experiments	Band sealing behavior observed
Takahashi et al. (2007)	Berea sandstone + clay	80	~2.5	0–100	1.0 μm/s	During experiments	Strong permeability drop with shear
Torabi et al. (2007)	Reservoir analog sandstone	5–20	109.75–1097.6	0	81 μm/s	After experiments by analysis thin sections (porosity)	Anisotropic strain localization
Cuisiat and Skurtveit (2010)	Baskarp sand and Troll field offshore clay	0.7–10.5	~220	Sand-clay interbed	None reported	During experiments	Clay smear and sealing behavior observed
Kimura et al. (2020)	Tohoku silica sand	0.5–8.0	None reported	0–9.2	0.2–100 mm/min	After experiments	Analyze shearing velocity and effective normal stress
Zhang et al. (2019)	Sand-clay mixtures	10–40	~17	~4–26	0.3–100 μm/s	None reported	Critical threshold near 15% clay
Jiang et al. (2024)	Artificially cemented siltstone	0–3	20.94–248.71	10	50 μm/s	After experiments by tests	Band-permeability coupling and evolutionary process

tape measures, compasses, cameras, portable permeability meters or permeameters. While it may be reasonable to conduct macro-scale measurements for assessing the dimensions of deformation bands (especially with advancements in UAV measurement technology), measuring their physical properties directly in the field could introduce substantial errors. Hence, sampling these deformation bands for subsequent laboratory analysis might be considered. Although this approach may exhibit elements of random sampling when dealing with widely distributed deformation bands, it represents an optimal alternative to experimental simulation.

5.2. Measurements of petrophysical properties

Measurements of petrophysical properties of deformation bands in the field are less accurate, whereas measurements of geological samples in the laboratory are more reliable. Specifically, conducting tests on samples under confining and pore pressures enhances accuracy. The regular measurement of porosity and permeability data for the shear zone in ring shear experiments represents significant progress. However, experiments conducted on loose sediments saturated with water may be overly idealistic and not commonly observed in field or underground core studies. Similarly, performing ring shear experiments on consolidated rock simulates deformation bands and allows for coring operations to test the porosity and permeability of individual deformation bands, which is crucial for observing and analyzing variations in physical properties resulting from different conditions.

5.3. Image analysis technique

The description and analysis of deformation bands at the microscopic level primarily rely on thin sections and SEM image analysis. However, due to the extinction effect of quartz and feldspar, thin sections are less effective for observation compared to cast thin sections. Additionally, the cost of SEM is higher than that of producing cast thin sections. Nevertheless, both SEM and thin sections have a production flaw in which wear can occur during sample preparation, resulting in missing particles and matrix within the deformation band as well as cracks around it. These factors can significantly impact the analysis and description of deformation bands, particularly when working with a limited number of samples. For instance, cracks may be mistakenly associated with deformation bands. Therefore, ensuring the integrity of both thin sections and SEM images is crucial for accurate deformation band analysis.

The conventional analysis of images primarily focuses on the structural characteristics, such as size, morphology, boundary width (i.e., deformation band thickness), and the cataclastic particles surrounding the deformation band or shear zone. Qualitative analysis remains a key component alongside measurements of particle thickness and size. However, with advancements in interdisciplinary technology, tools like Image J are now employed to quantitatively analyze parameters including particle size, roundness, arrangement direction, and porosity within the deformation band. This integration has significantly enhanced the accuracy of image analysis. Notably, comparing these characteristics with those of the host rock can effectively highlight changes in both structure and physical properties within the deformation band. Given that ring shear experiments can simulate formation processes for such bands, this analytical approach holds great significance in comprehending their formation and development under various experimental conditions.

5.4. 3D model analysis technique

3D model analysis technique is concurrently advancing alongside the development of 2D model image analysis techniques. This advancement is evident in two aspects: firstly, the utilization of 3D models to comprehend the structural and morphological characteristics of deformation bands; secondly, the application of 3D models to assess the impact of deformation bands on fluid flow. The first model proves highly beneficial in comprehending the spatial distribution of deformation bands (Fig. 11(a) and (b)), which cannot be observed through outcrops or thin sections alone. It aids in constructing a comprehensive stereoscopic conceptual model. To enhance the accuracy and credibility of the conceptual 3D modeling (Fig. 11(a) and (b)), high-resolution, non-destructive imaging was employed to reconstruct the internal pore and throat structures of deformation band samples. Core samples collected from field exposures or experimental deformation setups were scanned using a Phoenix Nanotom S nano-CT system (GE Measurement & Control, Germany). The acquired CT datasets were subsequently processed using Volume Graphics Studio Max and Avizo 8.0 software for image segmentation, visualization, and pore-scale modeling. Unlike conventional methods such as mercury intrusion porosimetry, nano-CT imaging causes no physical damage to the sample and preserves the microstructure, which is essential for accurately capturing the pore-throat geometry within deformation bands. The scanning principle is analogous to mathematical integration, in which the cylindrical rock sample is virtually sliced into thousands of cross-sectional images. However, due to the fixed beam geometry and scanning from center to edge, the outermost slices are subject to geometric distortion (e.g., elliptical deformation), which can introduce some edge-related bias in quantitative analysis. Following image acquisition, a standardized workflow was applied: (1) subvolume selection targeting

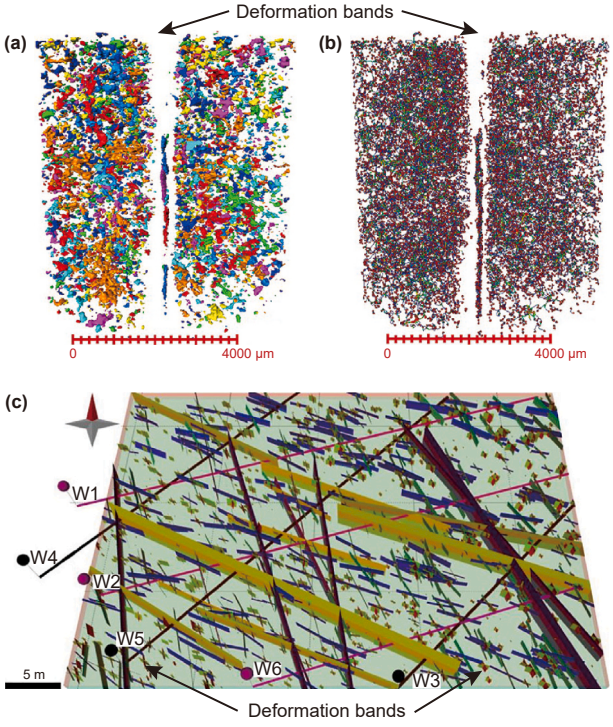

Fig. 11. Numerical models of deformation bands. **(a)** Pore-connected body model between deformation bands and host rock. **(b)** Pore-stick body model between deformation bands and host rock. **(c)** Distribution model of deformation bands and host rock, modified from Antonellini et al. (2014).

porous zones, (2) noise reduction via spatial filtering, (3) binary segmentation of solid and void phases, (4) pore space reconstruction through voxel filling, and (5) generation of a stereoscopic digital rock model. These models serve as the basis for further quantification of pore-throat network connectivity and morphological parameters within deformation bands. The second model integrates actual reservoir parameters and simulates how deformation bands influence fluid flow (Fig. 11(c)). While numerous studies have explored the effects of fractures on fluid flow through 3D modeling, few have considered the influence exerted by deformation bands. In most cases, these bands impede fluid flow and can even act as seals for oil and gas accumulations. Therefore, it is crucial to pay sufficient attention to and conduct thorough research on reservoir models that account for deformation band impacts. In the previous study (Antonellini et al., 2014), conceptual representations of deformation bands were translated into volumetric flow models by assigning distinct permeability and porosity attributes to grid cells intersected by these structures. To realistically capture their impact, a stochastic geometry-based approach was employed to populate the model domain with representative deformation band parameters, including orientation, aperture, intensity, and aspect ratio, calibrated from outcrop observations and literature-based analogues.

The geo-cellular model was discretized using a uniform mesh with a cell size of 0.2 m $\times$ 0.2 m $\times$ 0.5 m, consistent with the structural resolution required to resolve narrow, high-aspect-ratio bands. Flow simulations were performed using the MODFLOW 2005 engine, interfaced through ModelMuse, with flow governed by Darcy's law under steady-state conditions. Boundary conditions included fixed head on one side and no-flow boundaries on the lateral and basal surfaces. The solver was finite-difference-based, which ensures computational efficiency in large-scale models. Hydraulic properties such as anisotropic permeability tensors were assigned to different structural elements based on upscaled field measurements and analog permeability datasets. Although full experimental validation was beyond the scope of this conceptual demonstration, the results align with empirical observations of flow compartmentalization in band-rich sandstones. Future work should incorporate core-scale permeability measurements and tracer tests to calibrate and validate model outputs, thereby improving prediction accuracy for hydrocarbon recovery or CO_2 injection performance in deformation-band-influenced reservoirs.

In general, the measurement of deformation bands has transitioned from the field exploration stage to the laboratory research stage. However, in experiments, the analysis technology for deformation bands should not be limited to microscopic qualitative descriptions but should gradually incorporate interdisciplinary techniques such as ImageJ for quantitative analysis of particle size, circularity, arrangement direction, and porosity within the deformation band. Making full use of experimental results is crucial for comprehending various characteristics exhibited by deformation bands under different experimental conditions.

In developing these 3D numerical models, several simplifying assumptions were adopted to balance computational feasibility with structural resolution. Boundary conditions were fixed-head on one side and no-flow on the lateral and basal surfaces, which idealize reservoir-scale heterogeneity and may underrepresent cross-boundary fluid exchange. Fluid properties (e.g., density and viscosity) were assumed constant, neglecting potential temperature- or pressure-induced variations during subsurface flow. The rock matrix was treated as mechanically static during flow simulation, without accounting for possible deformation–permeability feedbacks. While these assumptions facilitate model convergence and permit clear isolation of deformation band effects, they also imply that the results should be interpreted as first-order trends rather than precise field predictions. Future work integrating variable fluid properties, more complex boundary conditions, and coupled hydro-mechanical processes would enhance model realism.

6. Future prospects

6.1. Challenges in experiments: In-situ permeability testing for consolidated rocks

The main experimental materials used in physical simulation experiments are loose sediments (Cuisiat and Skurtveit, 2010; Kimura et al., 2020). In the past, direct shear experiments with consolidated rock as the research object have been able to achieve in-situ permeability testing. However, due to instrument complexity, ring shear experiments can only be conducted with loose sediment as the object and not with consolidated rock (Fig. 12(a) and (b)). Currently, there is a lack of physical simulation experiments on deformation bands formed by consolidated rocks, and no reference exists on how to preserve these bands for analysis and testing purposes. Meanwhile, the existing apparatus cannot take the heating situation into account like the heated duct experiment (Al-Dulaimi and Hamad, 2023). Considering that various factors control the formation and evolution of cataclastic deformation bands under actual geological conditions (such as effective normal stress, shear displacement, clay content, mineral composition of host rock), further discussion is needed on conducting in-situ porosity and permeability characteristics analysis under different influencing factors or sample groups in order to establish a quantitative model for deformation characteristics and sealing ability.

6.2. Challenges in analysis: quantitative analysis technique

The traditional method of characterizing deformation bands only considers a single factor and mainly describes the structure from the perspective of thin section observation or particle size, shape, etc (Fig. 12(c) and (d)) (Pizzati et al., 2020). It fails to provide a complete quantitative analysis of the structure, such as quantifying the matrix formed by cataclasis or particle orientation. Therefore, solving how to quantitatively analyze structural characteristics under different influencing factors is crucial for analyzing formation and evolution.

6.3. Challenges in cementation: selection and utilization of cements

Previous physical simulation experiments did not take into account the presence of cement, which can significantly affect the deformation process depending on the amount and type of cement present in the host rock (Fig. 12(e) and (f)). The multi-stage or late cementation process and other diagenetic processes in clastic or carbonate rocks may greatly influence the structure and physical properties of deformation bands, but there is a lack of corresponding experimental studies to explore this phenomenon. Choosing an appropriate cementing agent is a complex matter that has not been addressed in previous experiments. The focus should be on whether the chosen cement will react with minerals from which deformation bands are formed. If no reaction occurs, epoxy resin appears to be one of the best choices based on pilot experiments; however, if a reaction does occur, determining an appropriate ratio and type of cement becomes challenging.

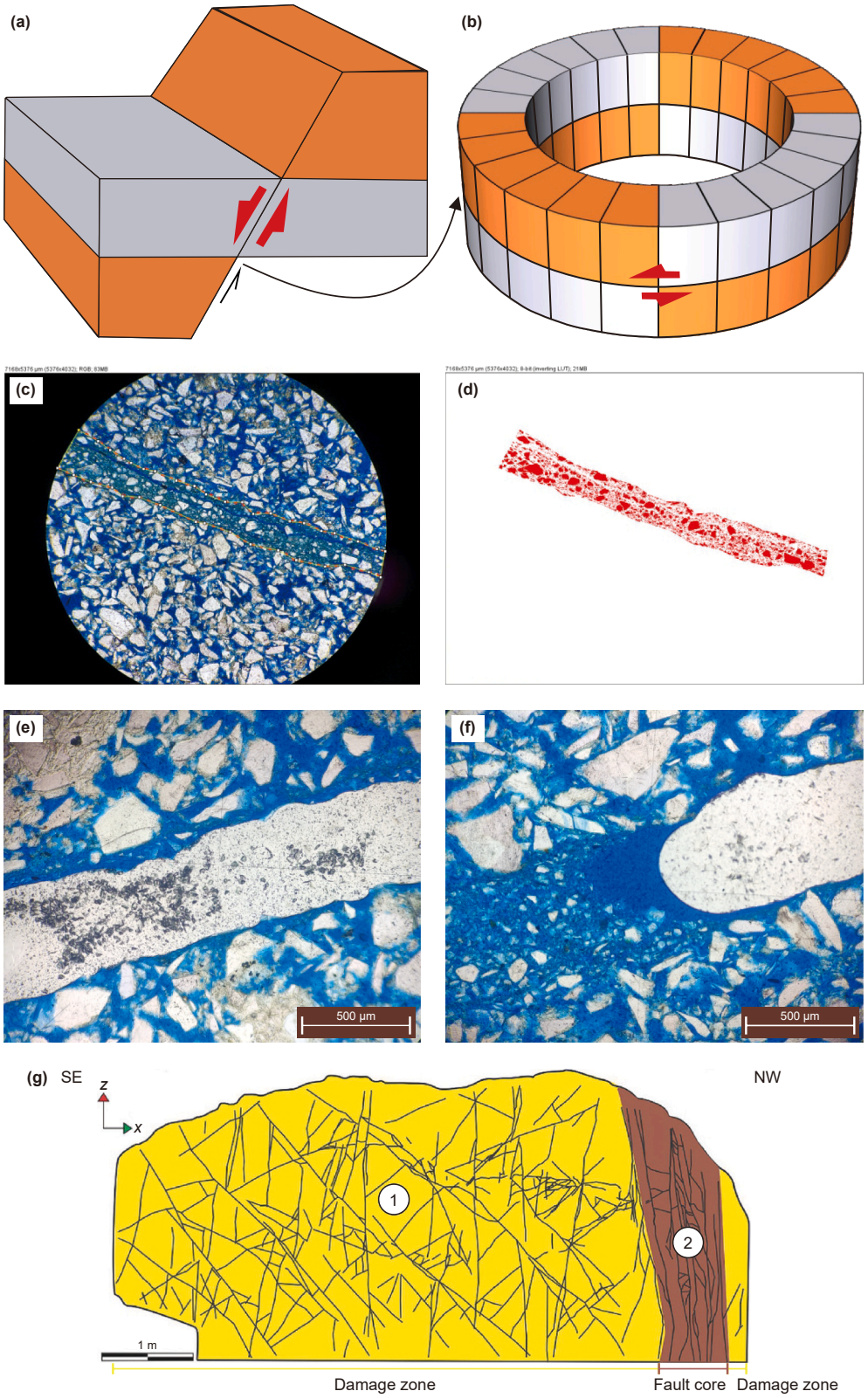

Fig. 12. Challenges in deformation band research. **(a)** Stratigraphic model and its corresponding **(b)** ring-shear test model, modified from Jiang et al. (2024). **(c)** Thin section and **(d)** its quantitative structural analysis, modified from Jiang et al. (2023). **(e)** Deformation band with complete cement infilling, modified from Jiang et al. (2026). **(f)** Deformation band with partial cement infilling, modified from Jiang et al. (2026). **(g)** Numerical simulation model of deformation bands, modified from Freitas et al. (2023).

6.4. Challenges in modeling: numerical simulation model

Although physical simulation experiments are a valuable method for studying deformation bands, they come with high material and economic costs. The parameters and results obtained from these experiments can be utilized to construct numerical simulation models (Fig. 12(g)). In the past, there has been extensive research on the correlation between fractures and faults in reservoir modeling, resulting in abundant data on their properties. However, when it comes to modeling deformation bands, the available data is not comprehensive enough and lacks necessary parameters. In other words, until the structural and physical properties of deformation bands are thoroughly quantitatively evaluated and the corresponding formation conditions are clearly understood, accurate numerical simulation modeling of deformation bands cannot be achieved.

6.5. Challenges in application: setting and application of the model

Physical simulation experiments are an essential approach for systematically studying the structure and physical properties of deformation bands. However, it is crucial not to confine the experimentation of deformation bands solely to a theoretical level. When designing experimental models, integrating conceptual models with simulated target strata to conduct comprehensive experiments can be considered. Additionally, it is necessary to contemplate how to obtain or carry out actual rock samples from different clay contents, host rock minerals, and stratifications in conjunction with artificial core samples for relevant physical simulations. While analyzing the results of experimental models, attention must be given to the fact that experimental simulations cannot be simply extrapolated for practical applications. It is imperative to elucidate both commonalities and differences between ring shear experiments and actual faulting processes while comparing sedimentary tectonic environments. Subsequently, based on this analysis, one can explain the application of experimental results.

The methodological advances synthesized in this review, particularly the development of a ring shear apparatus capable of testing consolidated rocks at centimeter-scale displacements, the integration of quantitative image analysis techniques, and the refinement of parameter control for key factors such as effective normal stress and shear displacement, provide a robust experimental foundation for addressing the future research directions outlined above. These advances establish a direct technical basis for tackling the identified challenges in in-situ permeability measurement, cementation simulation, and coupled hydro-mechanical modeling. By explicitly linking the proposed research avenues to demonstrated experimental capabilities, the future work envisioned in this study is anchored in proven methodological feasibility, thereby ensuring that subsequent investigations can build on existing laboratory achievements to generate insights with direct relevance to field applications.

In general, future research on deformation bands holds significant value and warrants further exploration. How can in-situ permeability testing be realized in physical simulation experiments using consolidated rock as the experimental object? How can all characteristics of deformation bands be quantitatively analyzed? How should cement be selected and utilized to simulate the formation process of deformation bands? How can an accurate numerical simulation model incorporating deformation bands be constructed? How can the deformation band model be correlated with actual formations to predict reservoir physical properties and fault sealing? These questions form the foundation for further investigation into the influence of deformation bands on fluid flow.

In addition to the key technical and methodological challenges discussed above, future research should also aim to integrate deformation band studies with broader geoscientific and energy-related applications. For example, the coupling of deformation band evolution with basin-scale hydrocarbon migration models, CO_2 geological storage feasibility assessments, and induced seismicity prediction frameworks will greatly enhance the applied relevance of this field. Furthermore, collaborative efforts combining experimental work, field data acquisition, machine learning analysis, and high-resolution geophysical imaging could offer a holistic perspective on fault-related heterogeneities. These interdisciplinary approaches will not only deepen the understanding of deformation mechanisms, but also extend the applicability of deformation band research to subsurface resource development, carbon neutrality strategies, and geohazard mitigation.

7. Concluding remarks

In the past, limited understanding of the qualitative structural and physical characteristics derived from actual deforming processes and key influencing factors has hindered progress in deformation bands research. A clearer understanding of the current status and advances in experimental simulation is therefore essential to address these challenges effectively. This paper aims to analyze the influence of key influencing factors on the structure and physical properties of deformation bands, compare the advantages and disadvantages of common experimental methods, identify issues existing in deformation band analysis methods, as well as discuss future challenges and potential improvements. The main points are outlined below:

(1) A significant number of outcrops and experimental studies on deformation bands indicate that, in terms of the formation, structure, and physical properties of these bands under similar geological conditions (including lithology, particle size, sorting, and porosity), the primary factors influencing their structure and physical properties are effective normal stress, shear displacement, strain rate, clay content, and host rock mineral composition. Among these factors, effective normal stress and shear displacement are the two most crucial considerations that should be taken into account during experimentation.
(2) Through the course of time, scholars have successfully addressed various challenges in the field, including but not limited to clay smear observation, stress loading control, millimeter displacement control, mechanical and permeability testing, as well as fluid sealing. The advent of ring shear experimental instruments specifically designed for consolidated rocks has facilitated experimental research on deformation bands with centimeter-scale displacement. Consequently, this advancement effectively resolves issues that have persisted over the past decade.
(3) The analytical technology for studying deformation bands in the laboratory should not be limited to qualitative descriptions at the micro level, but rather gradually incorporate interdisciplinary techniques such as ImageJ for quantitative analysis of particle size, circularity, arrangement direction, and porosity within the deformation band. Making optimal use of experimental results is crucial for comprehending the diverse characteristics exhibited by deformation bands under varying experimental conditions.

We Carry out physical simulation experiments using consolidated rock as the experimental subject, in order to investigate the

quantitative analysis of various factors on the structure and physical properties of deformation bands. Additionally, we restore and analyze the actual formation process of deformation bands, which serves as a fundamental basis for further research on their impact on fluid flow. Deformation bands find extensive applications in remaining oil development, fault sealing, reserve evaluation, gas storage site selection and operation, CO_2 geological storage, among others. Therefore, future research on deformation bands holds significant value and is worthy of exploration.

CRediT authorship contribution statement

Ming-Ming Jiang: Writing – review & editing, Writing – original draft, Visualization, Project administration, Methodology, Investigation, Funding acquisition, Conceptualization. **Xiao-Fei Fu:** Writing – review & editing, Writing – original draft, Resources. **Quan-You Liu:** Writing – review & editing, Writing – original draft, Supervision.

Declaration of competing interest

The authors declare that they have no known competing financial interests or personal relationships that could have appeared to influence the work reported in this paper.

Acknowledgements

This work was supported by the National Natural Science Foundation of China (Grant Nos. 42302146, 42488101, U25B6026-4), the Peking University-BHP Carbon and Climate Wei-Ming PhD Scholars Program (WM202503), the 2024 AAPG Foundation Grants-in-Aid, and China National Petroleum Corporation & Peking University Basic Research Project (JTGS2022JS327). Additionally, we extend our appreciation to the reviewers for their valuable contributions towards improving this paper.

Appendix A. Supplementary data

Supplementary data to this article can be found online at https://doi.org/10.1016/j.petsci.2025.09.029.

References

Al-Dulaimi, M.J., Hamad, F., 2023. Experimental investigation of the turbulence generators on heat transfer inside heated duct. Babyl. J. Mech. Eng. 2023, 71–77. https://doi.org/10.58496/bjme/2023/009.

Ali, A., Zaky, K.S., Wagreich, M., et al., 2022. Factors affecting the development of deformation bands in the Nubian Sandstone, Central Eastern Desert, Egypt. J. Afr. Earth Sci. 192, 104573. https://doi.org/10.1016/j.jafrearsci.2022.104573.

Alkhasli, S., Zeynalov, G., Shahtakhtinskiy, A., 2022. Quantifying occurrence of deformation bands in sandstone as a function of structural and petrophysical factors and their impact on reservoir quality: An example from outcrop analog of Productive series (Pliocene), South Caspian Basin. J. Pet. Explor. Prod. Technol. 12 (7), 1977–1995. https://doi.org/10.1007/s13202-021-01448-z.

Antonellini, M., Aydin, A., Orr, L., 1999. Outcrop-aided characterization of a faulted hydrocarbon reservoir: Arroyo Grande oil field, California, USA. Geophys. Monogr. 113, 7–26. https://doi.org/10.1029/GM113p0007.

Antonellini, M., Cilona, A., Tondi, E., et al., 2014. Fluid flow numerical experiments of faulted porous carbonates, Northwest Sicily (Italy). Mar. Petrol. Geol. 55, 186–201. https://doi.org/10.1016/j.marpetgeo.2013.12.003.

Araujo, R.E., Bezerra, F.H., Nogueira, F.C., et al., 2018. Basement control on fault formation and deformation band damage zone evolution in the Rio do Peixe Basin, Brazil. Tectonophysics 745, 117–131. https://doi.org/10.1016/j.tecto.2018.08.011.

Aydin, A., 1978. Small faults formed as deformation bands in sandstone. Pure Appl. Geophys. 116 (4–5), 913–930. https://doi.org/10.1007/978-3-0348-7182-2_22.

Aydin, A., Johnson, A.M., 1978. Development of faults as zones of deformation bands and as slip surfaces in sandstone. Pure Appl. Geophys. 116 (4), 931–942. https://doi.org/10.1007/BF00876547.

Aydin, A., Reches, Z., 1982. Number and orientation of fault sets in the field and in experiments. Geology 10 (2), 107–112. https://doi.org/10.1130/0091-7613(1982)10<107:NAOOFS>2.0.CO;2.

Ballas, G., Soliva, R., Sizun, J.P., et al., 2012. The importance of the degree of cataclasis in shear bands for fluid flow in porous sandstone, Provence, France. AAPG Bull. 96 (11), 2167–2186. https://doi.org/10.1306/04051211097.

Ballas, G., Soliva, R., Sizun, J.P., et al., 2013. Shear-enhanced compaction bands formed at shallow burial conditions; implications for fluid flow (Provence, France). J. Struct. Geol. 47, 3–15. https://doi.org/10.1016/j.jsg.2012.11.008.

Ballas, G., Fossen, H., Soliva, R., 2015. Factors controlling permeability of cataclastic deformation bands and faults in porous sandstone reservoirs. J. Struct. Geol. 76, 1–21. https://doi.org/10.1016/j.jsg.2015.03.013.

Balsamo, F., Storti, F., 2010. Grain size and permeability evolution of soft-sediment extensional sub-seismic and seismic fault zones in high-porosity sediments from the Crotone basin, southern Apennines, Italy. Mar. Petrol. Geol. 27, 822–837. https://doi.org/10.1016/j.marpetgeo.2009.10.016.

Balsamo, F., Storti, F., 2011. Size-dependent comminution, tectonic mixing, and sealing behavior of a "structurally oversimplified" fault zone in poorly lithified sands: Evidence for a coseismic rupture? GSA Bull. 123 (3–4), 601–619. https://doi.org/10.1130/B30099.1.

Balsamo, F., Pizzati, M., Nogueira, C., et al., 2024. Fault permeability in porous sandstone reservoirs: A short review of controlling factors. In: 85th EAGE Annual Conference & Exhibition (Including the Workshop Programme). European Association of Geoscientists & Engineers, pp. 1–6. https://doi.org/10.3997/2214-4609.2024101784.

Barla, G., Barla, M., Martinotti, M.E., 2010. Development of a new direct shear testing apparatus. Rock Mech. Rock Eng. 43 (1), 117–122. https://doi.org/10.1007/s00603-009-0041-5.

Baud, P., Klein, E., Wong, T., 2004. Compaction localization in porous sandstones: Spatial evolution of damage and acoustic emission activity. J. Struct. Geol. 26, 603–624. https://doi.org/10.1016/j.jsg.2003.09.002.

Beeler, N.M., Tullis, T.E., Blanpied, M.L., et al., 1996. Frictional behavior of large displacement experimental faults. J. Geophys. Res. 101 (B4), 8697–8715. https://doi.org/10.1029/96JB00411.

Berg, S.S., Skar, T., 2005. Controls on damage zone asymmetry of a normal fault zone: Outcrop analyses of a segment of the Moab fault, SE Utah. J. Struct. Geol. 27, 1803–1822. https://doi.org/10.1016/j.jsg.2005.04.012.

Berge, R.L., Gasda, S.E., Keilegavlen, E., et al., 2022. Impact of deformation bands on fault-related fluid flow in field-scale simulations. Int. J. Greenh. Gas Control 119, 103729. https://doi.org/10.1016/j.ijggc.2022.103729.

Braathen, A., Petrie, E., Nystuen, T., et al., 2020. Interaction of deformation bands and fractures during progressive strain in monocline - san Rafael Swell, Central Utah, USA. J. Struct. Geol. 141, 104219. https://doi.org/10.1016/j.jsg.2020.104219.

Brandes, C., Tanner, D.C., Fossen, H., et al., 2022. Disaggregation bands as an indicator for slow creep activity on blind faults. Commun. Earth Environ. 3, 99. https://doi.org/10.1038/s43247-022-00423-8.

Caine, J.S., Evans, J.P., Forster, C.B., 1996. Fault zone architecture and permeability structure. Geology 24, 1025. https://doi.org/10.1130/0091-7613(1996)024<1025:FZAAPS>2.3.CO;2.

Chemenda, A.I., Ballas, G., Soliva, R., 2014. Impact of a multilayer structure on initiation and evolution of strain localization in porous rocks: Field observations and numerical modeling. Tectonophysics 631, 29–36. https://doi.org/10.1016/j.tecto.2014.01.021.

Cheung, C.S.N., Baud, P., Wong, T., 2012. Effect of grain size distribution on the development of compaction localization in porous sandstone. Geophys. Res. Lett. 39. https://doi.org/10.1029/2012GL053739.

Childs, C., Walsh, J., Watterson, J., 1997. Complexity in fault zone structure and implications for fault seal prediction. Geol. Soc. Lond. Spec. Publ. 7, 61–72. https://doi.org/10.1016/S0928-8937(97)80007-0.

Childs, C., Walsh, J.J., Manzocchi, T., et al., 2007. Definition of a fault permeability predictor from outcrop studies of a faulted turbidite sequence, Taranaki, New Zealand. Geol. Soc. Lond. Spec. Publ. 292 (1), 235–258. https://doi.org/10.1144/SP292.14.

Childs, C., Manzocchi, T., Walsh, J.J., et al., 2009. A geometric model of fault zone and fault rock thickness variations. J. Struct. Geol. 31, 117–127. https://doi.org/10.1016/j.jsg.2008.08.009.

Choi, J.-H., Edwards, P., Ko, K., et al., 2016. Definition and classification of fault damage zones: A review and a new methodological approach. Earth Sci. Rev. 152, 70–87. https://doi.org/10.1016/j.earscirev.2015.11.006.

Chuhan, F.A., Kjeldstad, A., Bjørlykke, K., et al., 2003. Experimental compression of loose sands: Relevance to porosity reduction during burial in sedimentary basins. Can. Geotech. J. 40 (5), 995–1011. https://doi.org/10.1139/t03-050.

Cilona, A., Baud, P., Tondi, E., et al., 2012. Deformation bands in porous carbonate grainstones: Field and laboratory observations. J. Struct. Geol. 45, 137–157. https://doi.org/10.1016/j.jsg.2012.04.012.

Clausen, J.A., Gabrielsen, R.H., 2002. Parameters that control the development of clay smear at low stress states: An experimental study using ring-shear apparatus. J. Struct. Geol. 24, 1569–1586. https://doi.org/10.1016/S0191-8141(01)00157-2.

Compton, K.E., Kirkpatrick, J.D., Holk, G.J., 2017. Cyclical shear fracture and viscous flow during transitional ductile-brittle deformation in the Saddlebag Lake Shear Zone, California. Tectonophysics 708, 1–14. https://doi.org/10.1016/j.tecto.2017.04.006.

Cooke, A.P., Fisher, Q.J., Michie, E.A.H., et al., 2018. Investigating the controls on fault rock distribution in normal faulted shallow burial limestones, Malta, and the implications for fluid flow. J. Struct. Geol. 114, 22–42. https://doi.org/10.1016/j.jsg.2018.05.024.

Crawford, B.R., 1998. Experimental fault sealing: Shear band permeability dependency on cataclastic fault gouge characteristics. Geol. Soc. Lond. Spec. Publ. 127 (1), 27–47. https://doi.org/10.1144/GSL.SP.1998.127.01.04.

Crawford, B.R., Faulkner, D.R., Rutter, E.H., et al., 2001. Influence of clay content on strength, permeability and microstructure of synthetic quartz: Kaolinite fault gouge. In: AGU Fall Meeting Abstracts, p. T12G, 05.

Crawford, B., Myers, R., Woronow, A., et al., 2002. Porosity-permeability relationships in clay-bearing fault gouge. In: SPE/ISRM Rock Mechanics Conference. https://doi.org/10.2118/78214-MS.

Crawford, B.R., Faulkner, D.R., Rutter, E.H., 2008. Strength, porosity, and permeability development during hydrostatic and shear loading of synthetic quartz-clay fault gouge. J. Geophys. Res. 113 (B3), B03207. https://doi.org/10.1029/2006JB004634.

Cuisiat, F., Skurtveit, E., 2010. An experimental investigation of the development and permeability of clay smears along faults in uncemented sediments. J. Struct. Geol. 32, 1850–1863. https://doi.org/10.1016/j.jsg.2009.12.005.

Davies, R.K., Knipe, R.J., Souque, C., et al., 2009. Predicting fault Zone Architecture in the subsurface from outcrop analogues and the expected impact on flow. In: 2nd EAGE International Conference on Fault and Top Seals - from Pore to Basin Scale 2009. https://doi.org/10.3997/2214-4609.20147175.

de Melo Freitas, R.B.R., Nogueira, F.C.C., Vasconcelos, D.L., et al., 2023. 3D topological analysis in deformation bands: Insights for structural characterization and impact on permeability. J. Struct. Geol. 176, 104959. https://doi.org/10.1016/j.jsg.2023.104959.

De Souza, F.M., Gomes, I.F., Nogueira, F.C.C., et al., 2022. 2D modeling and simulation of deformation bands' effect on fluid flow: Implications for hydraulic properties in siliciclastic reservoirs. J. Struct. Geol. 158, 104581. https://doi.org/10.1016/j.jsg.2022.104581.

De Souza, D.H.S., Nogueira, F.C.C., Vasconcelos, D.L., et al., 2021. Growth of cataclastic bands into a fault zone: A multiscalar process by microcrack coalescence in sandstones of Rio do Peixe Basin, NE Brazil. J. Struct. Geol. 146, 104315. https://doi.org/10.1016/j.jsg.2021.104315.

Del Sole, L., Antonellini, M., Soliva, R., et al., 2020. Structural control on fluid flow and shallow diagenesis: Insights from calcite cementation along deformation bands in porous sandstones. Solid Earth 11 (6), 2169–2195. https://doi.org/10.5194/se-11-2169-2020.

Dewhurst, N., M, D., Jones, R., 2002. Geomechanical, microstructural, and petrophysical evolution in experimentally reactivated cataclasites: Applications to fault seal prediction. AAPG Bull. 86 (8), 1383–1405. https://doi.org/10.1306/61EEDCA6-173E-11D7-8645000102C1865D.

Dimitrova, R.S., Yanful, E.K., 2012. Factors affecting the shear strength of mine tailings/clay mixtures with varying clay content and clay mineralogy. Eng. Geol. 125, 11–25. https://doi.org/10.1016/j.enggeo.2011.10.013.

Du Bernard, X., Labaume, P., Darcel, C., et al., 2002. Cataclastic slip band distribution in normal fault damage zones, Nubian sandstones, Suez rift. J. Geophys. Res. Solid Earth 107 (B7). https://doi.org/10.1029/2001JB000493. ETG 6-1-ETG 6-12.

Du, X., Jin, Z., Zeng, L., et al., 2023a. Characteristics and controlling factors of natural fractures in deep lacustrine shale oil reservoirs of the Permian Fengcheng Formation in the Mahu Sag, Junggar Basin, China. J. Struct. Geol. 175, 104923. https://doi.org/10.1016/j.jsg.2023.104923.

Du, X., Jin, Z., Zeng, L., et al., 2023b. Formation of natural fractures and their impact on shale oil accumulation in the Mahu Sag, Junggar Basin, NW China. Int. J. Coal Geol. 279, 104385. https://doi.org/10.1016/j.coal.2023.104385.

Elkhoury, J.E., Niemeijer, A., Brodsky, E.E., et al., 2011. Laboratory observations of permeability enhancement by fluid pressure oscillation of in situ fractured rock. J. Geophys. Res. 116 (B2), B02311. https://doi.org/10.1029/2010JB007759.

Engelder, J.T., 1974. Cataclasis and the generation of fault gouge. GSA Bull. 85 (10), 1515–1522. https://doi.org/10.1130/0016-7606(1974)85<1515:CATGOF>2.0.CO;2.

Exner, U., Grasemann, B., 2010. Deformation bands in gravels: Displacement gradients and heterogeneous strain. J. Geol. Soc. 167 (5), 905–913. https://doi.org/10.1144/0016-76492009-076.

Exner, U., Kaiser, J., Gier, S., 2013. Deformation bands evolving from dilation to cementation bands in a hydrocarbon reservoir (Vienna Basin, Austria). Mar. Petrol. Geol. 43, 504–515. https://doi.org/10.1016/j.marpetgeo.2012.10.001.

Fang, Y., Elsworth, D., Wang, C., et al., 2017. Frictional stability-permeability relationships for fractures in shales. J. Geophys. Res. Solid Earth 122 (3), 1760–1776. https://doi.org/10.1002/2016JB013435.

Fisher, Q.J., Knipe, R.J., 2001. The permeability of faults within siliciclastic petroleum reservoirs of the North Sea and Norwegian Continental Shelf. Mar. Petrol. Geol. 18, 1063–1081. https://doi.org/10.1016/S0264-8172(01)00042-3.

Fisher, Q.J., Casey, M., Harris, S.D., et al., 2003. Fluid-flow properties of faults in sandstone: The importance of temperature history. Geology 31 (11), 965. https://doi.org/10.1130/G19823.1.

Fisher, Q.J., Haneef, J., Grattoni, C.A., et al., 2018. Permeability of fault rocks in siliciclastic reservoirs: Recent advances. Mar. Petrol. Geol. 91, 29–42. https://doi.org/10.1016/j.marpetgeo.2017.12.019.

Flodin, E., Prasad, M., Aydin, A., 2003. Petrophysical constraints on deformation styles in Aztec Sandstone, Southern Nevada, USA. Pure Appl. Geophys. 160 (9), 1589–1610. https://doi.org/10.1007/s00024-003-2377-1.

Fossen, H., 2010. Structural Geology. Cambridge University Press, Cambridge, New York. https://doi.org/10.1017/CBO9780511777806.

Fossen, H., Bale, A., 2007. Deformation bands and their influence on fluid flow. AAPG Bull. 91 (12), 1685–1700. https://doi.org/10.1306/07300706146.

Fossen, H., Cavalcante, G.C.G., 2017. Shear zones – a review. Earth Sci. Rev. 171, 434–455. https://doi.org/10.1016/j.earscirev.2017.05.002.

Fossen, H., Hesthammer, J., 2000. Possible absence of small faults in the Gullfaks Field, northern North Sea: Implications for downscaling of faults in some porous sandstones. J. Struct. Geol. 22, 851–863. https://doi.org/10.1016/S0191-8141(00)00013-4.

Fossen, H., Schultz, R.A., Shipton, Z.K., et al., 2007. Deformation bands in sandstone: A review. J. Geol. Soc. 164 (4), 755–769. https://doi.org/10.1144/0016-76492006-036.

Fossen, H., Soliva, R., Ballas, G., et al., 2018. A review of deformation bands in reservoir sandstones: Geometries, mechanisms and distribution. Geol. Soc. Lond. Spec. Publ. 459 (1), 9–33. https://doi.org/10.1144/SP459.4.

Fu, X., Jiang, M., Hu, Z., et al., 2024. Quantification of factors affecting fault sealing by using machine learning: Shuangtaizi fault anticline, southern margin of the Liaohe Western depression, Northeastern China. Mar. Petrol. Geol. 168, 106999. https://doi.org/10.1016/j.marpetgeo.2024.106999.

Fukuoka, H., Sassa, K., Wang, G., et al., 2006. Observation of shear zone development in ring-shear apparatus with a transparent shear box. Landslides 3 (3), 239–251. https://doi.org/10.1007/s10346-006-0043-2.

Fukuoka, H., Sassa, K., Wang, G., 2007. Influence of shear speed and normal stress on the shear behavior and shear zone structure of granular materials in naturally drained ring shear tests. Landslides 4 (1), 63–74. https://doi.org/10.1007/s10346-006-0053-0.

Gibson, R.G., 1994. Fault-zone seals in siliciclastic strata of the Columbus Basin, offshore Trinidad. AAPG Bull. 78 (9), 1372–1385. https://doi.org/10.1306/A25FECA7-171B-11D7-8645000102C1865D.

Giger, S.B., Clennell, M.B., Harbers, C., et al., 2011. Design, operation and validation of a new fluid-sealed direct shear apparatus capable of monitoring fault-related fluid flow to large displacements. Int. J. Rock Mech. Min. Sci. 48 (7), 1160–1172. https://doi.org/10.1016/j.ijrmms.2011.09.005.

Giger, S.B., Clennell, M.B., Çiftçi, N.B., et al., 2013. Fault transmissibility in clastic-argillaceous sequences controlled by clay smear evolution. AAPG Bull. 97 (5), 705–731. https://doi.org/10.1306/10161211190.

Gong, L., Gao, S., Liu, B., et al., 2021a. Quantitative prediction of natural fractures in shale oil reservoirs. Geofluids 2021 (1), 5571855. https://doi.org/10.1155/2021/5571855.

Gong, L., Wang, J., Gao, S., et al., 2021b. Characterization, controlling factors and evolution of fracture effectiveness in shale oil reservoirs. J. Petrol. Sci. Eng. 203, 108655. https://doi.org/10.1016/j.petrol.2021.108655.

Gong, L., Liu, K., Ju, W., 2023. Editorial: advances in the study of natural fractures in deep and unconventional reservoirs. Front. Earth Sci. 10, 1096643. https://doi.org/10.3389/feart.2022.1096643.

Gong, L., Qin, X., Lu, J., et al., 2024. Fractures development characteristics and distribution prediction of carbonate buried hills in Nanpu Sag, Bohai Bay Basin, China. J. Nat. Gas Geosci. 9 (6), 417–430. https://doi.org/10.1016/j.jnggs.2024.10.001.

Hennings, P., Allwardt, P., Paul, P., et al., 2012. Relationship between fractures, fault zones, stress, and reservoir productivity in the Suban gas field, Sumatra, Indonesia. AAPG Bull. 96 (4), 753–772. https://doi.org/10.1306/08161109084.

Hesthammer, J., Fossen, H., 1999. Evolution and geometries of gravitational collapse structures with examples from the Statfjord Field, northern North Sea. Mar. Petrol. Geol. 16 (3), 259–281. https://doi.org/10.1016/S0264-8172(98)00071-3.

Hodson, K.R., Crider, J.G., Huntington, K.W., 2016. Temperature and composition of carbonate cements record early structural control on cementation in a nascent deformation band fault zone: Moab Fault, Utah, USA. Tectonophysics 690, 240–252. https://doi.org/10.1016/j.tecto.2016.04.032.

Ikari, M.J., Saffer, D.M., Marone, C., 2009. Frictional and hydrologic properties of clay-rich fault gouge. J. Geophys. Res. 114 (B05), B05409. https://doi.org/10.1029/2008JB006089.

Jiang, M., Fu, X., Shi, L., et al., 2022. Physical analogue experiment of microstructure and variation law of permeability within faults in HighPorosity sandstone. Earth Sci. 47 (5), 1805–1818. https://doi.org/10.3799/dqkx.2021.113 (in Chinese).

Jiang, M., Jin, Y., Fu, X., et al., 2023. The development of cataclastic bands in high-porosity sandstones: Insights from ring shear experiments. J. Struct. Geol. 175, 104952. https://doi.org/10.1016/j.jsg.2023.104952.

Jiang, M., Jin, Y., Fu, X., Liu, Q., 2026. Experimental and analytical approaches to deformation bands: A critical review of laboratory methods, quantitative techniques, and modeling strategies. Earth Sci. Rev. 272, 105343. https://doi.org/10.1016/j.earscirev.2025.105343.

Jiang, M., Fu, X., Wang, Z., 2024. An experimental investigation of the characteristics of cataclastic bands in high-porosity sandstones. GSA Bull. 136 (7–8), 3069–3084. https://doi.org/10.1130/B36801.1.

Jiang, M., Jin, Y., Hu, Z., 2025. Prediction and evaluation of fault lateral sealing ability: A new approach to integrating comprehensive controlling factors based on BP neural network. J. Earth Sci. https://doi.org/10.1007/s12583-025-0334-y.

Jin, Y., Meng, L., Lyu, D., et al., 2023. Risk assessment of fault reactivation considering the heterogeneity of friction strength in the BZ34-2 Oilfield, Huanghekou Sag, Bohai Bay Basin, China. Pet. Sci. 20 (5), 2695–2708. https://doi.org/10.1016/j.petsci.2023.06.007.

Kaproth, B.M., Kacewicz, M., Muhuri, S., et al., 2016. Permeability and frictional properties of halite-clay-quartz faults in marine-sediment: The role of

compaction and shear. Mar. Petrol. Geol. 78, 222–235. https://doi.org/10.1016/j.marpetgeo.2016.09.011.
Karakouzian, M., Hudyma, N., 2002. A new apparatus for analog modeling of clay smears. J. Struct. Geol. 24, 905–912. https://doi.org/10.1016/S0191-8141(01)00106-7.
Kimura, S., Kaneko, H., Ito, T., et al., 2014. The effect of effective normal stress on particle breakage, porosity and permeability of sand: Evaluation of faults around methane hydrate reservoirs. Tectonophysics 630, 285–299. https://doi.org/10.1016/j.tecto.2014.05.031.
Kimura, S., Kaneko, H., Noda, S., et al., 2018. Shear-induced permeability reduction and shear-zone development of sand under high vertical stress. Eng. Geol. 238, 86–98. https://doi.org/10.1016/j.enggeo.2018.02.018.
Kimura, S., Noda, S., Ito, T., et al., 2020. Experimental study of impact of shearing velocity and effective normal stress on post-shearing permeability evolution of silica fault gouges. Tectonophysics 789, 228521. https://doi.org/10.1016/j.tecto.2020.228521.
Klimczak, C., Schultz, R.A., 2013. Shear-enhanced compaction in dilating granular materials. Int. J. Rock Mech. Min. Sci. 64, 139–147. https://doi.org/10.1016/j.ijrmms.2013.08.012.
Klinkmüller, M., Schreurs, G., Rosenau, et al., 2016. Properties of granular analogue model materials: A community wide survey. Tectonophysics 684, 23–38. https://doi.org/10.1016/j.tecto.2016.01.017.
Labaume, P., Moretti, I., 2001. Diagenesis-dependence of cataclastic thrust fault zone sealing in sandstones. Example from the Bolivian Sub-Andean Zone. J. Struct. Geol. 23, 1659–1675. https://doi.org/10.1016/S0191-8141(01)00024-4.
Laubach, S.E., Zeng, L., Hooker, J.N., et al., 2023. Deep and ultra-deep basin brittle deformation with focus on China. J. Struct. Geol. 175, 104938. https://doi.org/10.1016/j.jsg.2023.104938.
Lindsay, N.G., Murphy, F.C., Walsh, J.J., et al., 1992. Outcrop studies of shale smears on fault surface. In: Flint, S.S., Bryant, I.D. (Eds.), The Geological Modelling of Hydrocarbon Reservoirs and Outcrop Analogues. Blackwell Publishing Ltd., Oxford, UK, pp. 113–123. https://doi.org/10.1002/9781444303957.ch6.
Liu, B., He, S., Meng, L., et al., 2021. Sealing mechanisms in volcanic faulted reservoirs in Xujiaweizi extension, northern Songliao Basin, northeastern China. AAPG Bull. 105 (8), 1721–1743. https://doi.org/10.1306/03122119048.
Liu, Z., Sun, Y., 2020. Characteristics and formation process of contractional deformation bands in oil-bearing sandstones in the Hinge of a fold: A case study of the Youshashan anticline, western Qaidam Basin, China. J. Petrol. Sci. Eng. 189, 106994. https://doi.org/10.1016/j.petrol.2020.106994.
Liu, Z., Fu, X., Deng, S., et al., 2021. The critical control of arkosic sandstone porosity on deformation band formation: Insights from the Shulu across-fault borehole in the Bohai Bay Basin, China. J. Struct. Geol. 143, 104258. https://doi.org/10.1016/j.jsg.2020.104258.
Lommatzsch, M., Exner, U., Gier, S., et al., 2015. Dilatant shear band formation and diagenesis in calcareous, arkosic sandstones, Vienna Basin (Austria). Mar. Petrol. Geol. 62, 144–160. https://doi.org/10.1016/j.marpetgeo.2015.02.002.
Ma, C., Zhan, H., Zhang, T., et al., 2019. Investigation on shear behavior of soft interlayers by ring shear tests. Eng. Geol. 254, 34–42. https://doi.org/10.1016/j.enggeo.2019.04.002.
Maerten, L., Gillespie, P., Daniel, J.M., 2006. Three-dimensional geomechanical modeling for constraint of subseismic fault simulation. AAPG Bull. 90 (9), 1337–1358. https://doi.org/10.1306/03130605148.
Main, I., Mair, K., Kwon, O., et al., 2001. Experimental constraints on the mechanical and hydraulic properties of deformation bands in porous sandstones: A review. Geol. Soc. Lond. Spec. Publ. 186 (1), 43–63. https://doi.org/10.1144/GSL.SP.2001.186.01.04.
Mair, K., Frye, K.M., Marone, C., 2002. Influence of grain characteristics on the friction of granular shear zones. J. Geophys. Res. 107 (B10), 4–9. https://doi.org/10.1029/2001JB000516. ECV 4-1-ECV.
Mandl, G., Jong, L.N.J., Maltha, A., 1977. Shear zones in granular material: An experimental study of their structure and mechanical genesis. Rock Mech. 9 (2–3), 95–144. https://doi.org/10.1007/BF01237876.
Matthäi, S.K., Aydin, A., Pollard, D.D., et al., 1998. Numerical simulation of departures from radial drawdown in a faulted sandstone reservoir with joints and deformation bands. Geol. Soc. Lond. Spec. Publ. 147 (1), 157–191. https://doi.org/10.1144/GSL.SP.1998.147.01.11.
Meng, L., Fu, X., Wang, Y., et al., 2014. Internal structure and sealing properties of the volcanic fault zones in Xujiaweizi Fault Depression, Songliao Basin, China. Petrol. Explor. Dev. 41 (2), 165–174. https://doi.org/10.1016/S1876-3804(14)60019-7.
Mozley, P.S., Goodwin, L.B., 1995. Patterns of cementation along a Cenozoic normal fault: A record of paleoflow orientations. Geology 23 (6), 539–542. https://doi.org/10.1130/0091-7613(1995)023<0539:POCAAC>2.3.CO;2.
Nicchio, M.A., Nogueira, F.C.C., Balsamo, F., et al., 2018. Development of cataclastic foliation in deformation bands in feldspar-rich conglomerates of the Rio do Peixe Basin, NE Brazil. J. Struct. Geol. 107, 132–141. https://doi.org/10.1016/j.jsg.2017.12.013.
Nicol, A., Childs, C., 2018. Cataclasis and silt smear on normal faults in weakly lithified turbidites. J. Struct. Geol. 117, 44–57. https://doi.org/10.1016/j.jsg.2018.06.017.
Noorsalehi-Garakani, S., Kleine Vennekate, G.J., Vrolijk, P., et al., 2013. Clay-smear continuity and normal fault zone geometry – first results from excavated sandbox models. J. Struct. Geol. 57, 58–80. https://doi.org/10.1016/j.jsg.2013.09.008.
Oda, M., Kazama, H., 1998. Microstructure of shear bands and its relation to the mechanisms of dilatancy and failure of dense granular soils. Geotechnique 48 (4), 465–481. https://doi.org/10.1680/geot.1998.48.4.465.
Oliveira, L.S.B., Nogueira, F.C.C., Vasconcelos, D.L., et al., 2022. Mechanical stratigraphy influences deformation band pattern in arkosic sandstones, Rio do Peixe Basin, Brazil. J. Struct. Geol. 155, 104510. https://doi.org/10.1016/j.jsg.2022.104510.
Parnell, J., Watt, G.R., Middleton, D., et al., 2004. Deformation band control on hydrocarbon migration. J. Sediment. Res. 74 (4), 552–560. https://doi.org/10.1306/121703740552.
Pei, Y., Paton, D.A., Knipe, R.J., et al., 2015. A review of fault sealing behaviour and its evaluation in siliciclastic rocks. Earth Sci. Rev. 150, 121–138. https://doi.org/10.1016/j.earscirev.2015.07.011.
Pei, Y., Paton, D.A., Knipe, R.J., et al., 2020. Field-based investigation of fault architecture: A case study from the Lenghu fold-and-thrust belt, Qaidam Basin, NE Tibetan Plateau. GSA Bull. 132 (1–2), 389–408. https://doi.org/10.1130/B35140.1.
Pickering, G., Peacock, D.C.P., Sanderson, D.J., et al., 1997. Modeling tip zones to predict the throw and length characteristics of faults. AAPG Bull. 81 (1), 82–99. https://doi.org/10.1306/522B4299-1727-11D7-8645000102C1865D.
Pizzati, M., Balsamo, F., Storti, F., 2020. Displacement-dependent microstructural and petrophysical properties of deformation bands and gouges in poorly lithified sandstone deformed at shallow burial depth (Crotone Basin, Italy). J. Struct. Geol. 137, 104069. https://doi.org/10.1016/j.jsg.2020.104069.
Rawling, G.C., Goodwin, L.B., 2003. Cataclasis and particulate flow in faulted, poorly lithified sediments. J. Struct. Geol. 25, 317–331. https://doi.org/10.1016/S0191-8141(02)00041-X.
Rotevatn, A., Fossen, H., 2011. Simulating the effect of subseismic fault tails and process zones in a siliciclastic reservoir analogue: Implications for aquifer support and trap definition. Mar. Petrol. Geol. 28, 1648–1662. https://doi.org/10.1016/j.marpetgeo.2011.07.005.
Rotevatn, A., Sandve, T.H., Keilegavlen, E., et al., 2013. Deformation bands and their impact on fluid flow in sandstone reservoirs: The role of natural thickness variations. Geofluids 13 (3), 359–371. https://doi.org/10.1111/gfl.12030.
Sadrekarimi, A., Olson, S.M., 2010. Shear band formation observed in ring shear tests on sandy soils. J. Geotech. Geoenviron. Eng. 136 (2), 366–375. https://doi.org/10.1061/(ASCE)GT.1943-5606.0000220.
Sammis, C., King, G., Biegel, R., 1987. The kinematics of gouge deformation. Pure Appl. Geophys. 125 (5), 777–812. https://doi.org/10.1007/BF00878033.
Samuelson, J., Elsworth, D., Marone, C., 2009. Shear-induced dilatancy of fluid-saturated faults: experiment and theory. J. Geophys. Res. 114 (B12), B12404. https://doi.org/10.1029/2008JB006273.
Schultz, R.A., 2019. Geologic Fracture Mechanics. Cambridge University Press, Cambridge. https://doi.org/10.1017/9781316996737.
Scibek, J., 2020. Multidisciplinary database of permeability of fault zones and surrounding protolith rocks at world-wide sites. Sci. Data 7 (1), 95. https://doi.org/10.1038/s41597-020-0435-5.
Sigda, J.M., Goodwin, L.B., Mozley, P.S., et al., 1999. Permeability alteration in small-displacement faults in poorly lithified sediments: Rio Grande Rift, Central New Mexico. In: Haneberg, W.C., Mozley, P.S., Moore, J.C., Goodwin, L.B. (Eds.), Geophysical Monograph Series. American Geophysical Union, pp. 51–68. https://doi.org/10.1029/GM113p0051.
Silva, M., Nogueira, F., Pérez, Y., et al., 2022. Permeability modeling of a basin-bounding fault damage zone in the Rio do Peixe Basin, Brazil. Mar. Petrol. Geol. 135, 105409. https://doi.org/10.1016/j.marpetgeo.2021.105409.
Skurtveit, E., Torabi, A., Alikarami, R., et al., 2015. Fault baffle to conduit developments: Reactivation and calcite cementation of deformation band fault in aeolian sandstone. Pet. Geosci. 21 (1), 3–16. https://doi.org/10.1144/petgeo2014-031.
Soliva, R., Ballas, G., Fossen, H., et al., 2016. Tectonic regime controls clustering of deformation bands in porous sandstone. Geology 44 (6), 423–426. https://doi.org/10.1130/G37585.1.
Solum, J.G., Brandenburg, J.P., Naruk, S.J., et al., 2010. Characterization of deformation bands associated with normal and reverse stress states in the Navajo Sandstone, Utah. AAPG Bull. 94 (9), 1453–1475. https://doi.org/10.1306/01051009137.
Takahashi, M., 2003. Permeability change during experimental fault smearing. J. Geophys. Res. Solid Earth 108 (B5), 2235. https://doi.org/10.1029/2002JB001984.
Takahashi, M., Mizoguchi, K., Kitamura, K., et al., 2007. Effects of clay content on the frictional strength and fluid transport property of faults. J. Geophys. Res. 112 (B8), B08206. https://doi.org/10.1029/2006JB004678.
Tesei, T., Carpenter, B.M., Giorgetti, C., et al., 2017. Friction and scale-dependent deformation processes of large experimental carbonate faults. J. Struct. Geol. 100, 12–23. https://doi.org/10.1016/j.jsg.2017.05.008.
Tikoff, B., Wojtal, S.F., 1999. Displacement control of geologic structures. J. Struct. Geol. 21, 959–967. https://doi.org/10.1016/S0191-8141(99)00045-0.
Tindall, S.E., 2006. Jointed deformation bands may not compartmentalize reservoirs. AAPG Bull. 90 (2), 177–192. https://doi.org/10.1306/08240505068.
Tindall, S.E., 2014. Simple calculations of fluid flow across jointed cataclastic deformation bands. Mar. Petrol. Geol. 57, 152–159. https://doi.org/10.1016/j.marpetgeo.2014.05.016.
Tindall, S., Eckert, A., 2015. Geometric and mechanical-stiffness controls on jointing in cataclastic deformation bands. J. Struct. Geol. 77, 126–137. https://doi.org/10.1016/j.jsg.2015.05.008.

Torabi, A., Braathen, A., Cuisiat, F., et al., 2007. Shear zones in porous sand: Insights from ring-shear experiments and naturally deformed sandstones. Tectonophysics 437 (1–4), 37–50. https://doi.org/10.1016/j.tecto.2007.02.018.

Torabi, A., Rudnicki, J., Alaei, B., et al., 2023. Envisioning faults beyond the framework of fracture mechanics. Earth Sci. Rev. 238, 104358. https://doi.org/10.1016/j.earscirev.2023.104358.

Tueckmantel, C., Fisher, Q.J., Manzocchi, T., et al., 2012. Two-phase fluid flow properties of cataclastic fault rocks: Implications for CO_2 storage in saline aquifers. Geology 40 (1), 39–42. https://doi.org/10.1130/G32508.1.

Wafid Agung, M., Sassa, K., Fukuoka, H., et al., 2004. Evolution of shear-zone structure in undrained ring-shear tests. Landslides 1 (2), 101–112. https://doi.org/10.1007/s10346-004-0001-9.

Wibberley, C.A.J., Petit, J.P., Rives, T., 1999. Mechanics of high displacement gradient faulting prior to lithification. J. Struct. Geol. 21, 7. https://doi.org/10.1016/S0191-8141(99)00006-1.

Yan, S., Qun, L., Jiang, Z., et al., 2021. Enrichment of tight oil and its controlling factors in central and western China. Petrol. Explor. Dev. 48 (2), 492–506. https://doi.org/10.1016/S1876-3804(21)60040-X.

Zeng, L., Gong, L., Guan, C., et al., 2022. Natural fractures and their contribution to tight gas conglomerate reservoirs: A case study in the northwestern Sichuan Basin, China. J. Petrol. Sci. Eng. 210, 110028. https://doi.org/10.1016/j.petrol.2021.110028.

Zhang, F., An, M., Zhang, L., et al., 2019. The role of mineral composition on the frictional and stability properties of powdered reservoir rocks. J. Geophys. Res. Solid Earth 124 (2), 1480–1497. https://doi.org/10.1029/2018JB016174.

Zhang, S., Tullis, T.E., Scruggs, V.J., 1999. Permeability anisotropy and pressure dependency of permeability in experimentally sheared gouge materials. J. Struct. Geol. 21, 795–806. https://doi.org/10.1016/S0191-8141(99)00080-2.

Zhu, R., Xie, W., Liu, Q., et al., 2022. Shear behavior of sliding zone soil of loess landslides via ring shear tests in the South Jingyang Plateau. Bull. Eng. Geol. Environ. 81 (6), 244. https://doi.org/10.1007/s10064-022-02719-7.